IONIC INTERACTIONS IN EMAA IONOMER BLENDS: A RHEOLOGICAL AND MECHANICAL PROPERTY INVESTIGATION

by

Marina Najm
B.A.Sc., The University of British Columbia, 2019

A THESIS SUBMITTED IN PARTIAL FULFILLMENT OF
THE REQUIREMENTS FOR THE DEGREE OF

MASTER OF APPLIED SCIENCE
in
THE FACULTY OF GRADUATE AND POSTDOCTORAL STUDIES
(Chemical and Biological Engineering)

THE UNIVERSITY OF BRITISH COLUMBIA
(Vancouver)

August 2021

The following individuals certify that they have read, and recommend to the Faculty of Graduate and Postdoctoral Studies for acceptance, a thesis entitled:

Ionic Interactions in EMAA Ionomer Blends: A Rheological and Mechanical Property Investigation

submitted by	Marina Najm	in partial fulfillment of the requirements for
the degree of	Master of Applied Science	
in	Chemical and Biological Engineering	

Examining Committee:

Dr. Savvas G. Hatzikiriakos, Chemical and Biological Engineering, UBC

Supervisor

Peter Englezos, Chemical and Biological Engineering, UBC

Supervisory Committee Member

Laurel Schafer, Chemistry, UBC

Supervisory Committee Member

Abstract

Polyethylene-co-methacrylic acid (EMAA) ionomers are functionalized polymers with up to 15% carboxylic acid groups neutralized by counterions such as sodium, zinc, or lithium. Due to the polarity difference between the polar cations and the nonpolar hydrocarbon chain, ionic groups aggregate into clusters which act as crosslinks leading to improved mechanical strength, viscosity, and self-healing properties. The analysis done in this study shows that binary mixtures of two different cations further enhance the rheological and mechanical properties such as complex viscosity, Young's modulus, and yield strength. The enhancement is beyond what is calculated through the linear combination of the corresponding properties of the individual components forming the blends. The morphological change supporting the synergism is suggested to be an increased cluster strength and phase segregation for highly neutralized EMAA ionomers. However, this synergism is not observed for large stresses and deformations outside the linear region due to the deformation of clusters as a stress-release mechanism. Investigation of interaction in binary ionic binary blends of EMAA ionomers is measured using linear, nonlinear, and extensional rheology in the melt state, and using dynamic mechanical tensile testing in the solid state. A universal parameter, the "Molecular weight-normalized Neutralization" (N_{MW}), is developed and found to be correlated to the presence of rheological and mechanical property enhancement for all binary blends. N_{MW} is composed of the inverse of molecular weight and of neutralization. High N_{MW} obtained through high degrees of combined cation neutralization and low combined molecular weight ionomers are correlated with higher degrees of enhancement. More significant synergism has been found for blends containing zinc counterions due to the high valency of their ionic charge compared to sodium or lithium counterions.

Lay Summary

Ionomers are polymers with a small fraction of ions which modify the mechanical and rheological properties of the precursor polymer chain. Their improved strength has made ionomers suitable for packaging, membranes, and coatings. This work investigates the effect of mixing two different ion types on the mechanical (e.g. stiffness) and rheological properties (e.g. viscosity). The main question is whether mixing two different ions leads to properties expected from the linear combination of those of the two individual components, or whether the ions interact to result in enhanced mechanical and rheological properties. It has been found that high concentrations of two different neutralizing cations lead to increased strength and rheological properties beyond those of the neat components. In addition, different parameters such as polymer chain size, ionic charge, and ionic concentration are analyzed to identify the most significant factor for ionic interactions for a material with a wider range of applications.

Preface

This work builds on previous analysis of the pure sodium and zinc ionomers published by M. Zuliki, S. Zhang, K. Nyamajaro, T. Tomkovic, S.G. Hatzikiriakos, "Rheology of sodium and zinc ionomers: Effects of neutralization and valency," Physics of Fluids, 32(2), (2020) and by T. Tomkovic, S.G. Hatzikiriakos, "Nonlinear rheology of poly(ethylene-co-methacrylic acid) ionomers," Journal of Rheology, 62 (6), (2018) . Melt state rheological testing of pure sodium ionomers were performed by T. Tomkovic. Methacrylic acid content and degree of neutralization measurements were performed by S. Zhang and K. Nyamajaro. Melt state rheological testing of pure zinc ionomers were performed by M. Zuliki.

This project focuses on the rheological and mechanical analysis of binary blends of sodium, zinc, and lithium ionomers. Most of the work discussed in chapter 3 has been submitted for publication under the title "Synergistic Ionic Interactions in EMAA Ionomer Blends: A Rheological and Mechanical Property Investigation" by M. Najm, B. Yavitt, and S.G. Hatzikiriakos. Essentially, a version of chapter 3 has been used to draft the submitted article listed above. Revisions were done by S.G Hatzikiriakos. Experimental design, blend preparation, testing of melt state rheology of lithium pure ionomers and of all ionomer blends, solid-state mechanical testing, as well as data analysis and the writing of this thesis and the manuscript for the submitted article were performed by the author of this Master thesis under the supervision of Professor S.G. Hatzikiriakos at the University of British Columbia. Feedback to refine the analysis of the rheological measurements including the comparison of linear versus nonlinear behavior and the formulation of molecular weight-normalized neutralization was provided by Dr. B. Yavitt. Two shear rheometers and a dynamic mechanical analyzer (DMA) in the Chemical and Biological Engineering department at the University of British Columbia were used by the author of this thesis to obtain the experimental measurements.

Table of Contents

List of Tables

List of Figures

List of Symbols

E_a	Activation energy
G'	Storage modulus
G''	Loss modulus
G_i	Maxwell relaxation modulus
M_w	Weight-average molecular weight
N_{MW}	Molecular weight-normalized Neutralization
T	Temperature
T_c	Crystallization Temperature
T_g	Glass Transition Temperature
T_m	Melting Temperature

List of Greek Symbols

γ	Strain
η^*	Complex viscosity
η_E^+	Tensile stress growth coefficient
λ_i	Relaxation time

List of Abbreviations

DSC	Differential Scanning Calorimetry
EMAA	Ethylene Methacrylic Acid
EXAFS	Extended X-ray Absorption Fine Structure Spectroscopy
FTIR	Fourier Transform Infrared Spectroscopy
LVE	Linear Viscoelasticity
MW	Molecular Weight
MAA	Methacrylic acid
SER	Sentmanat Extensional Rheometer
SHF	Strain Hardening Factor
THF	Tetrahydrofuran
tTS	Time-Temperature Superposition
XAS	X-ray Absorption Spwctroscopy

Acknowledgements

I would like to express sincere gratitude to my research supervisor Professor Savvas G Hatzikiriakos for his guidance, patience, and advice throughout my program. I am very grateful for all the opportunities he has sent my way, and for all the knowledge I have gained through the discussions we had.

I would also like to thank all members of the rheology group for the inspiring and entertaining conversations we had. I would like to thank Ben Yavitt for his feedback, constructive criticism, and for guiding my analysis into a more thorough and insightful work.

I would like to thank the NSERC CGS- M grant for funding my master program and for extending their financial support.

And finally, I would like to deeply thank my family who have been incredibly loving, supportive, and encouraging in every way.

Dedication

Dedicated to my family

Chapter 1: Introduction

To begin, an introduction on ionomers is provided, followed by their previously studied characteristics, rheological and mechanical properties. The objectives of this work and the organization of this document are then presented.

1.1 Definition, Characteristics, and Applications of Ionomers

Ionomers are thermoplastic polymers with a small fraction (15%) of acid groups covalently bonded to the backbone chain[1]. The term "ionomer" was first used by Rees from E. I. Dupont de Nemours & Co. describing the copolymer formed from ethylene and methacrylic acid[2]. Two widely used ionomers are Nafion® and Surlyn®, both developed by Dupont in the mid-1960s. Nafion ionomers have a polytetrafluoroethylene backbone with perfluorinated-vinyl-polyether side chains terminated by sulphonic acid end groups[3]. Their high temperature and electrochemical stability have allowed them to be the most common and commercially available materials for polymer electrolyte membranes, a core component of proton exchange membrane fuel cells, biological fuel cells, and direct methanol fuel cells[4,5]. Surlyn ionomers, the materials analyzed in this study, are a semi-crystalline copolymer of ethylene and methacrylic acid (EMAA) [6]. Carboxylate groups are the functional group covalently bonded to the polymer backbone. The carboxylate groups are then neutralized by either hydrogen (to form carboxylic acid) or by metal counterions to form the corresponding metal carboxylate group. For example, sodium counterions form sodium carboxylate, and lithium counterions form lithium carboxylate groups. Some other reported cations are calcium, zinc, and magnesium[7–11]. Thus, the carboxylate groups do not have a net charge in either of their forms. However, we will refer to the hydrogen-neutralized carboxylic acid groups as unneutralized, and to the metal-carboxylate groups as neutralized methacrylic acid groups, with the terminology referring to the metal counterion neutralizing the carboxylate group.

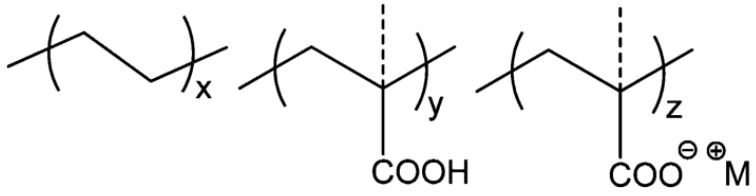

Figure 1.1 Molecular structure of ethylene methacrylic acid (EMAA) formed of copolymers of ethylene and methacrylic acid, and the carboxylic acid group neutralized by a positively charged counterion (M^+)[2]

Both the carboxylic acid groups and the neutralizing counterions bestow additional intermolecular interactions to the chain dynamics. First, the carboxylic acid groups form interchain monomer-dimer hydrogen bonds at room temperature in their unneutralized state[12] as shown in Figure 1.2.

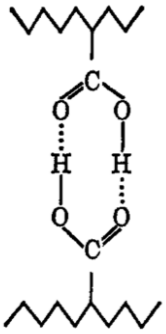

Figure 1.2 Schematic representation of interchain linking through carboxylic acid group dimer formation[12]

Once counterions are introduced, the weaker hydrogen bonds become insignificant as the stronger ionic associations control chain dynamics[13]. In addition, the polar neutralizing counterions form ionic clusters within the nonpolar hydrocarbon matrix and phase separate into nanoscale domains between 2 and 5 nm in size[14]. Neutralizing cations can be dispersed in the polymer matrix or aggregated in clusters depending on their concentration. For example, an X-ray absorption spectroscopy (XAS) study shows Zn ions isolated at neutralizations below 5% for 3.9 mol% MAA, and as aggregates at neutralization above 30%[15]. EMAA chains with carboxylic acid groups neutralized by isolated counterions or by ionic clusters have delayed dynamics due to the stronger bond between negatively charged COO^- and positively charged neutralizing cations which prevents chain relaxation. The ionic associations act as reversible crosslinks, improving the mechanical, optical, and self-healing properties of the base EMAA polymer[16]. These ionic associations once dissociated allow EMAA chains released from the ionic groups to undergo relaxation leading to flow within the hydrocarbon matrix until another available counterion is encountered to form another association[17]. This behavior is called "ion hopping"[18], where an ionomer chain diffuses from one ionic domain to another. The resulting neutralized ionomer has delayed relaxation and increased rheological and mechanical properties due to the presence of ionic crosslinks[19], yielding a material with increased rheological and

mechanical properties[20]. Since the acid content and neutralization degree are adjustable, ionomers have tunable properties beneficial for a wide variety of applications. Ionomers' high chemical, abrasion, and impact resistance are suitable for coating and sealing film applications, and their high toughness is suitable for packaging for several consumer products[2]. Furthermore, self-healing properties have also been studied and explained by an elastic recovery of the polymer chain followed by interdiffusion and sealing, even at temperatures below the melting temperature (T_m)[21].

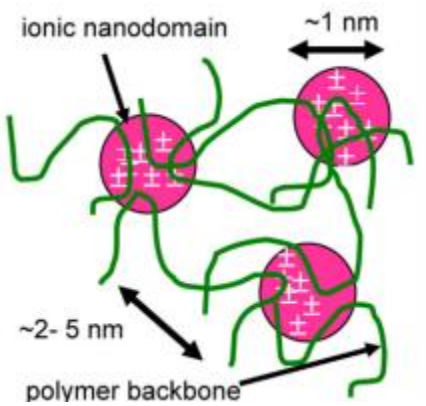

Figure 1.3 Schematic representation of ionic clusters within the polymer backbone matrix. ± represents the positively charged cations neutralizing the negatively charged acid groups covalently attached to the hydrocarbon chain[2]

More particularly, the strength and impact of ionic groups varies depending on their location in the ionic aggregate, such as in the center of the aggregate, at the edge of the aggregate, or as an isolated cation. Spectroscopy studies with Xray Absorbance Spectroscopy (XAS) reveal a general planar structure of ionic aggregates, with curvature to minimize free energy. Proposed structures for the three positions matching XAS patterns and considering steric hindrance are shown in Figure 1.4 for zinc as a counterion. Zinc is a transition metal able to form coordinate bonds with carboxylate oxygen groups leading to an ordered structure, unlike sodium ions which aggregate into disordered structures. Isolated Zn ions neutralize two carboxylates (Figure 1.4C), while aggregate Zn ions coordinate to four carboxylate groups (Figure 1.4A-aggregate interior, Figure 1.4B-aggregate edge)[22]. The arrangement of zinc aggregates remains unchanged over a wide range of temperatures up to 180ºC.[23] In fact, Nishioka et al refer to EMAA ionomers as terpolymers, with the three components being the ethylene backbone, the charged methacrylic acid groups, and the metal cation methacrylate that form upon neutralization and ionic clustering.

These three components each contribute to the rheological properties to a certain order of magnitude and at a different time scale, all to be considered during analysis[24].

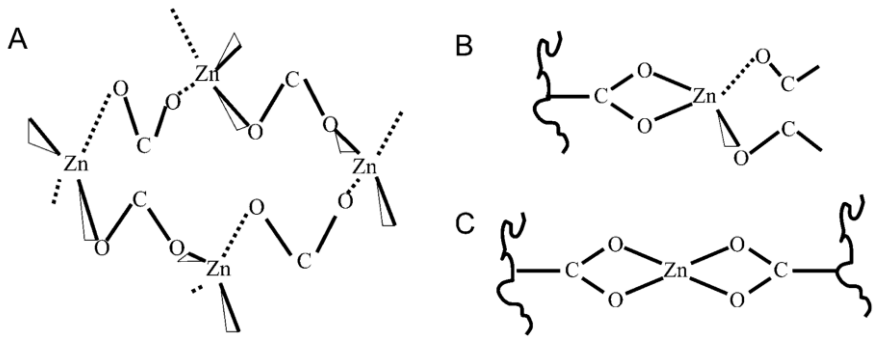

Figure 1.4 (A) Schematic for the anhydrous zinc structure inside the ionic aggregate which appears mostly planar, (B) zinc atoms at edges of ionic aggregates, and (C) isolated zinc ions forming coordinate bonds with two chelating carboxylates. Structures are proposed to match XAS patterns[22]

1.2 Effect of neutralizing counterions

A wide range of EMAA neutralizing cations besides zinc have been recorded in literature such as sodium, calcium, magnesium, and lithium[10,12,23,25]. The structure of ionic aggregates depends on the type of bonds that can be formed by each neutralizing cation. Transition metals such as zinc, titanium, cadmium, and iron can form coordinate bonds with the carboxylate oxygen groups. The resulting bonds have higher strength than those formed by alkali or alkaline earth metals such as sodium and lithium which do not form coordinate covalent bonds[22]. In addition, calcium counterions induce a larger increase in viscosity compared to sodium cations, a difference which remains up to high temperatures[10]. The onset of aggregation is also different for each cation, with Li, Mg, and Na forming ionic clusters at 35% while Zn clusters form at a neutralization of 80%[19]. The effects of ionic type, size, and valency on the resulting blend properties and synergism will be investigated in the following chapters.

1.3 Rheological Properties of Ionomers

To quantify the effects of ionic interactions as they relate to molecular structure, rheological experiments can be performed to relate the flow dynamics to the morphology. The rheological properties of polyethylene methacrylic acid (EMAA) ionomers have been studied extensively in the literature. The overall behavior of the ionomers is affected by the structure and the valency of the ions since multiplets behave as crosslinks reinforcing the polymer backbone[7]. This is

explained by the formation of aggregate metal conjugates at high ion concentrations which has been verified by multiple studies through spectroscopic, thermophysical, and rheological analysis[14,18,24,26,27]. Viscosity in the presence of counterions can increase by up to three orders of magnitude at full neutralization, which reduces the ease of processing for industrial or commercial applications[28]. Neutralization is therefore limited to lower levels (30-60%) to maintain processability without the need to use plasticizers. However, one factor that lowers viscosity is the presence of moisture. This leads to a reduction in melt viscosity due to the disruption of hydrogen bonds between non-neutralized methacrylic acid groups and due to the weakening of ionic interactions by dissolution of ions into absorbed water molecules. To mitigate these effects, ionomers are typically dried for several days.

Rheological testing can capture the chain relaxation dynamics by calculation of the average association and relaxation time, as well as the extent to which the EMAA chains relax compared to the full relaxation theoretically possible at the terminal relaxation time[29].
Multiple theories have been developed to model the dynamics of ionomers which fall under the class of associating polymers. Liebler et al.'s model of entangled networks with temporary crosslinks states that the system behaves as an elastic solid at times shorter than the lifetime of temporary crosslinks but is allowed to diffuse within the theoretical confining tube at longer time scales when the chain is released from the crosslinks[30]. Chen et al have developed the sticky Rouse model describing two relaxation modes. A rapid polymer relaxation occurs simultaneously with a 100x slower glassy relaxation due to ionic rearrangement[1]. Other models applicable to polymers in general such as the K-BKZ model[31] have also been applied to ionomers comparing elongational dynamics to shear dynamics, both enhanced by the presence of ionic clusters[8].

1.4 Mechanical Properties of Ionomers

The mechanical properties of EMAA ionomers have also been studied as a function of ion type and concentration[1,9,32–34]. EMAA ionomers are found to have higher stiffness and moduli and slower relaxation with the incorporation of neutralizing cations like sodium, zinc, and lithium. The stiffness of EMAA ionomers neutralized by K, Na, and Mg reaches a maximum at 33% neutralization, and at 70% for Zn counterions[19]. Since the formation of ionic clusters leads to

microphase separation and impedes ion-hopping (mechanism of ionomer flow) delaying chain relaxation, the tensile properties such as stiffness increase with ion incorporation. A further increase in solid state stiffness has been observed in blends of ionomers compared to those of the neat ionomer components[19].

1.5 Effect of binary blends of neutralizing counterions

Having reviewed the properties of pure ionomers through rheological and mechanical methods, ionomer blends have been proven to modulate desirable properties such as luminescent efficiency[35], dispersion[36], self-healing properties[37], and miscibility[38] of the two polymer components. Ionomer blends allow tuning the properties of generated materials to obtain properties not previously possible by using the neat ionomer alone. Ionomer blends have been successfully used as compatibilizers enhancing miscibility of two immiscible polymers. For example, adding 4-vinylpyridine promotes miscibility between poly(methyl methacrylate) (MMA) and polystyrene which formed immiscible blends[39]. In addition, ionomer blends can combine desirable properties from different materials for specialized applications. For instance, Dow has combined Surlyn blends with an additive to produce a hybrid golf ball coating with reduced energy dissipation for better spin and longer distance coverage[40]. Blends of poly(ethylene glycol-co-cyclohexane-1,4-dimethanol terephthalate) (PETG) gain self-healing properties after blending them with EMAA at a 50/50 ratio as a result of synergistic effects of chain mobility and new chemical interactions between PETG and EMAA[41]. EMAA ionomers have been combined into blends with montanic acid[25], lignin[36], polyethyleneimine[16], chlorinated polyethylene[33], acrylonitrile styrene acrylate (ASA)[42], styrene-butadiene-styrene (SBS)[37], aramid[43], and multiple fatty acids[44]. The blends of interest in this study are binary combinations of EMAA chains with different metal cations (Na/Zn, Zn/Li, Na/Li) as neutralizing cations. The blended EMAA backbones have different molecular weight, methacrylic acid content, cation type, and neutralization degrees. Thermal and spectroscopic analysis, such as DSC, FTIR, and extended X-ray absorption fine structure (EXAFS), has revealed the formation of conjugated metal salts for blends of Zn and Na in EMAA ionomers[24,26]. Tachino et al[26]. have also presented a clear enhancement in stiffness, tensile, and melt index of ionomers neutralized by two different cations. This enhancement is supported by FTIR analysis showing an additional absorbance peak not present in either the sodium or the zinc spectrum. However, no enhancement was

reported for high strain measurements or in any sample in the melt state at a temperature above 190°C due to the melting of both ionic and polyethylene crystallites[26]. However, Vanhoorne and Register claim that the ionic aggregates remain in the molten state up to 300°C[45]. No rigorous rheological investigation of possible enhancement by cation interactions has been reported for EMAA blends in the melt state.

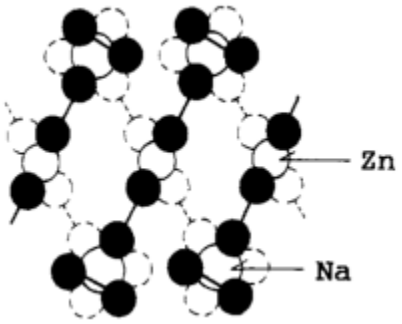

Figure 1.5 Schematic model for an ionic cluster formed by a conjugate sodium-zinc metal salt in an EMAA ionomer blend. Dotted circles represent oxygen atoms into the plane of the molecule, and dark circles represent oxygen atoms out of the plane of the molecule[26].

Grady[46] analyzed extended x-ray absorption fine structure (EXAFS) spectra of co-neutralized EMAA with both zinc and sodium cations showing the presence of multiple types of aggregates at all Zn/Na rations, with their relative distribution changing with the concentration of zinc cations. Low Zn/Na ratios allow the coexistence of both zinc and sodium in ionic aggregates which are reported to be weaker than pure zinc or pure sodium aggregates. Finally, Nishio et al[47]. have performed rheological studies revealing the influence of ion type on zero shear viscosity, but no discussion on synergistic effects of the blends. They attribute the change in viscosity values to the ability of the binary blend to undergo acid-cation exchange between the metal cation and the neutralizing hydrogen of the carboxylic acid group. Since sodium is stated to bond with COOH groups, exchange of Na^+ and H^+ ions is possible allowing for chain diffusion and accelerated relaxation. In contrast, zinc cations which neutralize carboxylate (COO^-) groups do not exhibit acid-cation exchange leading to delayed relaxation and increased viscosity[47]. Although multiple mechanisms are attributed to ionic aggregate structure and dynamics, no thorough reporting of rheological and mechanical properties for a range of blends has been presented. This study covers a range of neutralization degrees comparing the effects on

melt state rheology (linear and nonlinear behavior), effects on solid state behavior, as well as thermal and spectroscopic analyses.

1.6 Electrical Properties of Ionomers

Although not the focus of this study, electrical properties of EMAA ionomers are acknowledged. EMAA ionomers are poor conductors of electricity due to the low percentage of ionic components and to the low mobility of the charge conductors. EMAA ionomers have at most 15 mol % acid groups, which are not completely neutralized by counterions[48]. The large size of the cations along with their phase segregation and low mobility limit the conductivity of EMAA ionomers, leading to a conductivity between 10^{-10} and 10^{-6} $[\Omega\ cm]^{-1}$ [49]. On the other hand, sulfonated ionomers such as the polymer electrolyte membrane Nafion® is intrinsically conductive due to the large sulfonate pendant groups, stable fluorinated backbone, high ionic concentration and ionic diffusivity resulting in an average conductivity at least 4 orders of magnitude higher than that of EMAA, at $10^{-2} – 10^{-1}$ $[\Omega\ cm]^{-1}$ [50]. The poor conductivity of EMAA ionomers does not warrant an investigation into their electrical properties in this study.

1.7 Research Objectives

The goal of this work is to investigate the rheological and mechanical properties of binary mixtures of cations in ethylene methacrylic acid ionomer blends. Analysis will be performed on rheological studies of melt state linear and nonlinear shear deformation, melt state extensional rheological measurements, and solid-state tensile testing. The study will evaluate the effect of multiple parameters such as molecular weight, methacrylic acid content, neutralization, cation charge and valency, and blend ratio to elucidate conditions that favor enhancement of selected properties (synergism) beyond those that can be expected from the linear combination of the pure ionomers forming the blends. These parameters will be discussed using molecular and topological arguments to explain the changes in thermal, structural, rheological, and mechanical structure. An investigation comparing the multiple variables will aim to identify parameters with statistical significance in the presence and intensity of synergism to formulate a universal metric for comparing all tested blends with various composition parameters.

1.8 Thesis Organization

Chapter 1 introduces ionomer structure and characteristics, and the suitable applications based on their mechanical and rheological properties. A review of studies about EMAA ionomer rheology and structure is presented to establish the current state of research and to guide the analysis in subsequent chapters. The objectives of this research on EMAA ionomer blends are also presented in this chapter as well as the organization of this thesis.

Chapter 2 describes the materials and the equipment used for testing the ionomer blends to determine their thermal, rheological, and mechanical properties. The theory behind each measurement and analysis is also explained.

Chapter 3 provides a discussion on the experimental results and the analysis applied to all ionomer binary blends, explaining the changes in the local environment around ionic clusters associated with the observed changes in rheological and mechanical properties.

Chapter 4 concludes this thesis by summarizing the results and providing recommendations for applications of the formed blends as well as future analysis that can build upon the findings of this research.

Chapter 2: Materials, Equipment, and Methodology

This chapter presents the materials and methods used for blend preparation. The experimental equipment, methods used, and theory behind the thermal and molecular characterization as well as rheological and mechanical testing are also presented.

2.1 Materials

Generally, ionomers are synthesized in two steps. First, the polymer backbone is synthesized by copolymerization of acid groups and the precursor monomer, or by post-synthesis modification of the hydrocarbon chain to incorporate covalently bonded acid groups. EMAA copolymers are synthesized through free-radical polymerization of ethylene and methacrylic acid monomers. The polyethylene component maintains structural properties of low-density polyethylene, including a high degree of branching and polydispersity, while the methacrylic acid groups are randomly distributed, negatively charged components with the ability to form hydrogen bonds[17]. Addition of counterions is done through solution neutralization by dissolving the copolymer and metal salt in a solvent. The solvent is often a mixture of polar and nonpolar liquids to dissolve both the nonpolar hydrocarbon chain and the polar ionic and metal groups. Commercially, neutralization is done through melt mixing of the ionomer with a metal hydroxide[22].

For this study, partially neutralized Surlyn® poly(ethylene-co-methacrylic acid) ionomer pellets were provided by Dupont (Experimental Station, Wilmington, DE, USA). The backbone chain structure is a random copolymer of polydisperse branched polyethylene and methacrylic acid synthesized using free-radical polymerization[51]. Small angle X-ray spectroscopy (SAXS) reveals that the MAA groups are statistically distributed along the ethylene chain[45]. Ionomers are labeled as X-C Y where X is the mol percent of MAA, C is the cation, and Y is the degree of neutralization. For example, 7.2-Na 65 contains 7.2 mol % MAA, 65% of which are neutralized by sodium. Details on these ionomers such as acid content, degree of neutralization, molecular weight characteristics, zero shear viscosity (η_o), the energy of activation (E_{act}), and melting point, can be found in Table 2.1. The neutralizing ions are sodium, zinc, or lithium cations of varying concentration, and are shown in Table 2.2 for each blend. The solvents tetrahydrofuran (THF)

and m-xylene used to dissolve the ionomers to prepare the various blends were purchased from Sigma-Aldrich.

Table 2.1 Properties of ionomers used in the present study including commercial name, weight and mole % of MAA concentration, degree of neutralization, and molecular and rheological characteristics.

Ionomer	Surlyn®	wt % MAA	Mol % MAA	% Neutral	Mw (g/mol)	η_o 140°C (kPa.s)	E_{act} (kJ/mol)	T_m (°C)	Used in Blend #
1.5-Na 69	1601	4.3	1.5	69	72,500	86.4	87.3	99	3,6
1.6-Na 63	1605	4.9	1.6	63	114,500	55.4	81.9	96	2
4.1-Na 65	1707	11.5	4.1	65	71,000	176	90.3	94	8
7.2-Na 65	1802	19.2	7.2	65	65,200	33.9	79.3	99	1,4,7
3.4-Zn 40	9650	9.7	3.4	40	62,400	38	91.6	97	1
3.8-Zn 60	1650	10.8	3.8	60	81,900	58	87.4	93	3,5
5.9-Zn 33	9120	16.8	5.9	33	114,200	322	126.6	96	2,4
5.5-Li 40	7940	14.7	5.5	40	60,000	119	93.5	91	5,6,7,8

Table 2.2 Ionomer components for each binary blend of cations bound to EMAA chains. Mixing ratios of 20%, 50%, and 80% by mass were made for each blend.

Blend #	Zn	Na
1	3.4-Zn 40	7.2-Na 65
2	5.9-Zn 33	1.6-Na 63
3	3.8-Zn 60	1.5-Na 69
4	5.9-Zn 33	7.2-Na 65

Blend #	Zn	Na	Li
5	3.8-Zn 60		5.5-Li 40
6		1.5-Na 69	5.5-Li 40
7		7.2-Na 65	5.5-Li 40
8		4.1-Na 65	5.5-Li 40

2.2 Ionomer Blend Preparation

Ionomer pellets are weighed to obtain the desired mass ratio of the various blends, namely Zn/Na (blends 1-4), Zn/Li (blend 5), or Na/Li (blends 6-8) listed in Table 2.2. Three weight ratios by mass of 20%, 50%, and 80% binary mixtures for each blend are prepared to investigate the effect of cation ratio and degree of neutralization on cluster formation and thus on their rheological and mechanical properties. These mass ratios are selected to span the full range of the binary blend to locate the proportion that favors synergistic effects. Eight binary combinations are selected as

shown in Table 2.1 and Table 2.2 with 3 ratios each for a total of 24 prepared binary counterion blends, aside from the pure ionomer components. The weighed EMAA pellets of the two selected components are placed in a round-bottom flask with 95% THF / 5% m-xylene solvent and a magnetic stirrer (200 rpm). The flask is submerged in a water bath heated to 90°C to reach the boiling point of the THF solvent to accelerate the dissolution of the ionomeric pellets. The flask is connected to a reflux condenser to recirculate the evaporated THF/xylene. Other bath fluids such as silicone oil would be more suitable compared to water for a temperature of 90°C since water evaporates quickly. However, the pellets dissolve within 3 h during which the flask is still submerged under water. After complete dissolution of ionomeric pellets, the flask is left to cool down during which the remaining THF/xylene solution evaporates. The contents are removed from the flask, washed with methanol to remove the remaining solvent, and placed in a vacuum oven for at least 7 days at 75°C before testing to eliminate moisture and mitigate the reduction of rheological and mechanical properties as explained in the previous chapter[29]. Consequently, they are stored in a desiccator over $CaSO_4$.

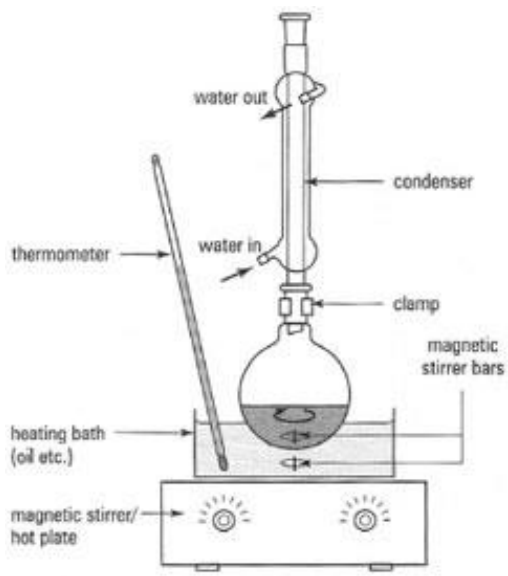

Figure 2.1 Schematic showing reflux condensation setup for solution melt mixing of ionomer blends [52]

The disks for rheological testing are prepared by compression molding the dried ionomer blend fragments at 170°C for 15 minutes at a minimal pressure to melt all contents. This is followed by the application of a pressure of 5MPa for 5 minutes. The disk is then allowed to cool to room

temperature. Disks of thickness 0.3 – 0.4 mm are formed, suitable for rheological shear and extensional measurements from which strips are also cut for mechanical (tensile) testing.

2.3 Differential Scanning Calorimetry (DSC)

Differential Scanning Calorimetry (DSC) allows the thermal characterization of ionomer blends giving insight to molecular structure and crystallinity variation across different binary mixtures. DSC is based on the measurement of the change in enthalpy of a sample as it is exposed to a controlled temperature program[53]. The thermal properties of selected samples were measured on a Netzsch DSC 214 Polyma differential scanning calorimeter. Analyses were performed in an inert atmosphere (nitrogen) with samples of approximately 5-10 mg in a ceramic pan. All analyses were conducted in duplicate. Samples were heated to 150°C with a heating rate of 10 °C /min. They were held isothermally at 150 °C for 5 min to eliminate any thermal history followed by gradual cooling to 30°C with a cooling rate of 10 °C /min. The samples were then reheated to 150 °C with a heating rate of 10 °C /min. The glass transition temperatures were determined from the second heating ramp. Blend 3 at all mixing ratios 0, 20%, 50%, 80%, and 100% Zn (with the balance being Na) is selected for DSC analysis to fully characterize the observed enhancement first seen in rheological testing.

The thermal properties of the samples such as melting temperature, crystallization temperature, and enthalpy of phase transition give insight into the structural and thermal response of different polymer blends. Crystallization temperature (T_c) is identified as the temperature of the highest peak during the second cooling cycle. Melting temperature (T_m) is identified as the temperature of the highest peak during the second heating cycle. Crystallinity can be calculated by the ratio of enthalpy of fusion of the ionomer sample to the heat of fusion of polyethylene crystallites of a 100% crystalline LPDE with a value of 290.4 J/g[54,55].

2.4 Fourier Transform Infrared Spectroscopy (FTIR)

FTIR spectroscopy is a technique used to identify the molecules and bonds present in a material. Wavelengths between 400 and 4000 cm^{-1} are selected as they span the range corresponding to molecular vibrations [56]. For ionomer blends, the absorbance peaks of interest are for carboxylate symmetric and asymmetric stretching bands, their height relative to other peaks, as well as the

presence of any new peaks not found in the spectra of the parent ionomers. FTIR spectra were recorded at room temperature on a Perkin Elmer FTIR equipped with an ATR accessory for direct measurement of polymeric materials. Blend 3 was selected for testing since it showed noticeable interaction in rheological and tensile testing. FTIR was performed for the pure ionomers, 1.5-Na 69, 3.8-Zn 60, and the 20%, 50% and 80% Zn/Na blend (with the percentage referring to Zn).

2.5 Shear Rheometry

Rheology is the study of flow and deformation of matter. Most polymers are non-Newtonian materials, with their rheological properties, such as viscosity, dependent on the rate of deformation. At low rates of deformation (low frequency), polymer chains have sufficient time to undergo relaxation, giving rise to viscous liquid-like behavior. Under these conditions, the loss modulus G'' has larger values than the storage modulus G'. At high rates of deformation (high frequency), the experimental measurement time is shorter than the chain relaxation time, leading to dominant elastic, solid-like behavior. In this case the storage modulus G' has larger values than the loss modulus G''. Concerning the amplitude of deformation, small strains that do not permanently alter the structure of the polymer lie within the linear viscoelastic region, while larger deformations which shear the chains to a non-reversible state lie within the nonlinear viscoelastic region. A strain sweep experiment which scans a range of strain amplitudes allows the determination of the linear region for each polymer.

Rheological testing of polymers is done in the melt state to measure the dynamic behavior at experimentally measurable time scales and to obtain properties relevant to polymer processing which is performed at conditions above the melting temperature T_m[57]. Shear testing was performed using an Anton Paar MCR 702 rheometer equipped with the cone-partitioned plate geometry which allows testing at high strain values while delaying the effect of edge fracture (25mm 4 degree cone angle, 8mm partitioned plate, 0.051mm gap)[58]. The top plate is sectioned into an 8mm plate connected to the transducer for measurement, and a surrounding stationary area that acts as a shield to buffer and delay the transmission of edge fracture effects into the sample area being measured.

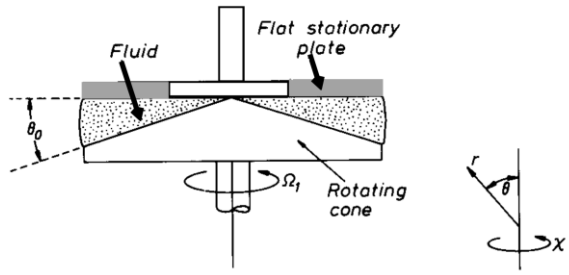

Figure 2.2 Schematic of cone and partitioned plate geometry showing the top parallel plate and stationary plate and bottom cone measuring system[59]. Figure modified to show sectioning of partitioned plate.

2.5.1 Small-Amplitude Oscillatory Shear

Frequency sweep tests were performed over the temperature range from 120°C to 180°C with 20°C increments at a strain amplitude of 5%, measured to be in the linear region using a strain sweep, and a frequency range between 0.01 – 100 rad/s at each of the four temperatures. The ionomers are thermally stable within this temperature range and for the whole duration of the experiments[29,60–63]. A reference temperature of 140°C was used for time-temperature superposition to generate the viscoelastic and viscosity master-curves for all samples. This is valid since all virgin ionomers have similar melting temperatures between 91-99°C, and the melting temperature of the blend is an intermediate linear combination of those of pure ionomers, verified by DSC. The error attributed to using the same reference temperature for all blends is expected to be minimal[64].

2.5.2 Stress Relaxation

Stress relaxation experiments to determine the linear and nonlinear relaxation modulus versus time were obtained over a shear strain range of 0.05 to 10 at 140°C. The measured relaxation moduli are a function of time and strain amplitude, giving insight to a maintained chain structure versus flow under deformation and to the ability of the chain to store elastic energy[65]. The damping coefficients are the values required to shift each relaxation modulus curve at each strain amplitude back to the reference curve which was obtained under conditions of linear strain. These damping coefficients are fitted into the Wagner (exponential) damping function[66] calculated as the ratio of strain-dependent relaxation modulus to the linear, strain-independent relaxation modulus,

$$h(\gamma) = \frac{G(\gamma,t)}{G(t)} = \frac{\alpha}{\alpha+\gamma^2} = \frac{1}{1+\frac{\gamma^2}{\alpha}} \qquad (1)^{66}$$

The damping function will be used as a measure of cluster formation and stability, and thus a way of checking for synergistic effects in the case of various blends.

2.6 Extensional Rheometry

Another nonlinear rheological measurement performed to detect synergistic effects is uniaxial extensional testing using the second generation Sentmanat extensional fixture (SER2, see Figure 2.3). This geometry is used to apply a constant extensional strain rate to a polymer strip in the melt state and measure the torque by which the extensional viscosity is then calculated. Strips having a width of 6mm and a thickness between 0.3 and 0.4mm were tested at Hencky strain rates of 0.5, 2, and 5 s^{-1} at 140°C. The resulting tensile stress growth coefficient, (transient extensional viscosity) was divided by the linear extensional viscosity of $3\eta^{+}$ to obtain the strain hardening factor (SHF). The SHF is a normalized parameter used to assess and identify synergistic effects.

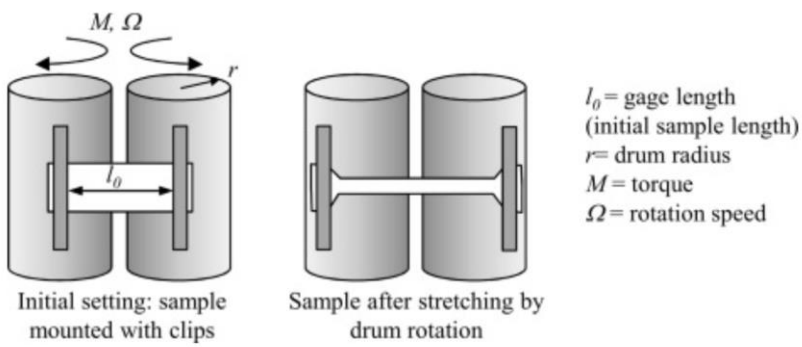

Figure 2.3 Schematic drawing of SER geometry for uniaxial extensional testing of polymer melts[57]

2.7 Mechanical Testing

In contrast to the previously discussed measurement techniques, mechanical testing is performed on ionomer samples in the solid state for property characterization and to evaluate whether ionic aggregates provide the same enhancement in the solid state as they do in the melt state. This is also relevant to commercial applications to determine the stability of aggregates over a wider temperature range. The solid-state tensile properties of the samples were measured using an RSA G2 TA Instruments Dynamic Mechanical Analyzer using the tensile fixture (Figure 2.4). Samples of 7 mm width, 0.3-0.4 mm thickness, and 15 mm length were held at 75°C for 3 min to equilibrate thermally and were subsequently stretched at a linear rate of 10mm/min. The selected

temperature of 75°C between crystallization temperature T_c (50-60°C) and melting temperature T_m (90-99°C) is chosen to maintain the solid state and ordering of ionic aggregates yet allow for the deformation of the ethylene hydrocarbon chain during testing. The initial slope of the stress versus strain curve is calculated to obtain the Young's modulus (Figure 2.5). The stress at the end of the linear deformation region is extracted as the yield stress (Figure 2.5). The stress at 100% strain is also compared to assess the effect of ionic aggregation on elongation at a common strain for all samples.

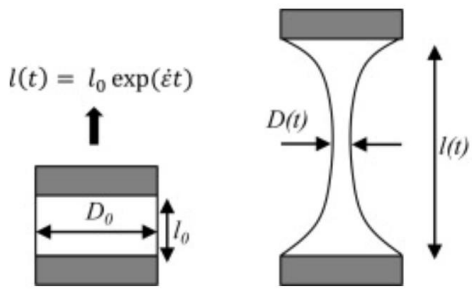

Figure 2.4 Schematic of tensile testing of polymer films showing necking upon deformation[57]

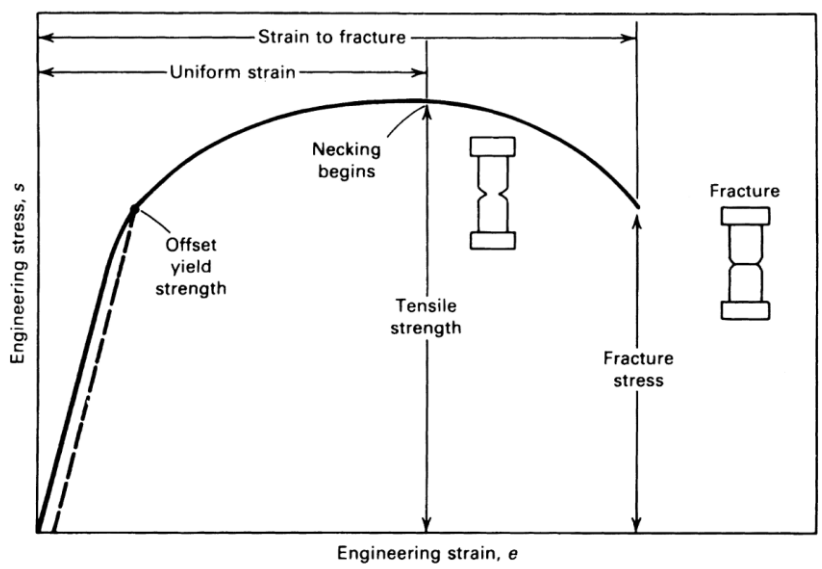

Figure 2.5 Stress vs strain curve for tensile testing of a solid polymer sample showing initial linear deformation, the limit of plastic deformation, necking, and fracture[67].

In summary, this chapter has described sample preparation and testing methods whose results will be discussed in the next section.

Chapter 3: Results and Discussion

This chapter discusses the results of the rheological and mechanical property experiments presented in the previous chapter. The measured thermal, rheological, and mechanical properties are analyzed considering synergism, neutralization, and ionic interaction.

3.1 Thermal Characterization

The amplitude and width of DSC exotherm peaks provide insight into the ordering of ionic clusters and can be related and helpful to rheological analysis. Measured thermograms are depicted in Figure 3.1 for blend 3 (see Table 2.2) composed of 3.8-Zn 60 and 1.5-Na 69. The melting temperature (T_m) of pure ionomers and blends are around 90°C and the corresponding crystallization temperature (T_c) at around 55°C, which agree well with reported values in the literature for this class of ionomers[26]. The exact variation of T_m and T_c are plotted in Figure 3.2.

The exotherm (crystallization) and endotherm (melting) peaks move to lower temperatures with increasing Zn content which is due to the lower melting point of Zn ionomers[63]. The wider exotherm peaks seen for increasing Zn/Na ratio suggests less ordering of Zn clusters and a disruption of cluster formation compared to the blends with higher monovalent Na content which show a narrower exotherm peak[68,69]. The 20%Zn/80%Na blend has the narrowest exothermic peak, which is correlated with a higher degree of ordering in ionic clusters (Figure 3.2). This blend composition which has the highest exotherm peak also exhibits the highest degree of neutralization as seen from FTIR (discussed in the following section), and the largest enhancement in rheological properties such as storage and loss moduli, complex viscosity, activation energy, and zero-shear viscosity in the melt state (discussed below in detail).

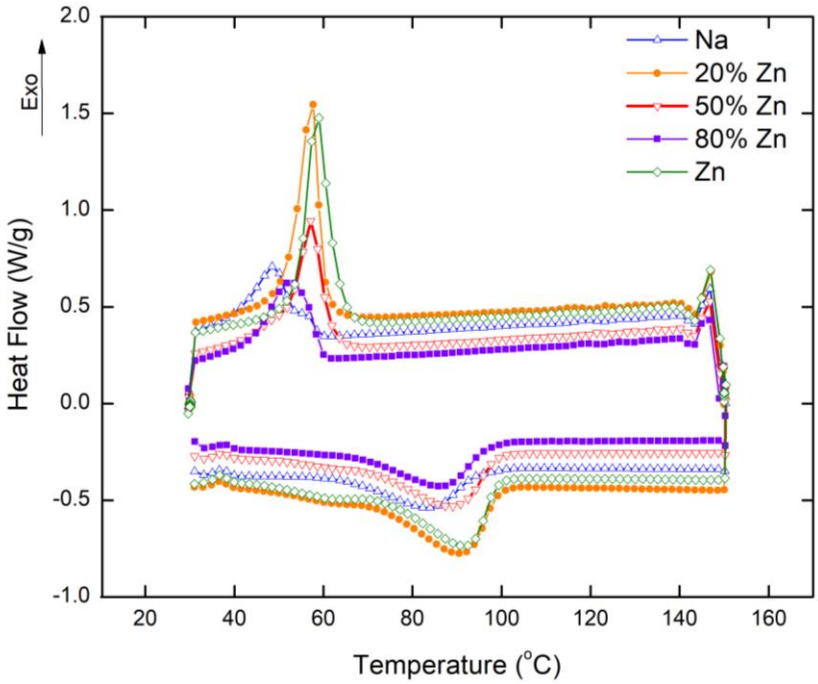

Figure 3.1 The second heating (lower endotherm) and cooling cycles (upper exotherm) of DSC results for all ratios of Blend 3 (see Table 2) that is blends of 3.8-Zn 60/1.5-Na 69.

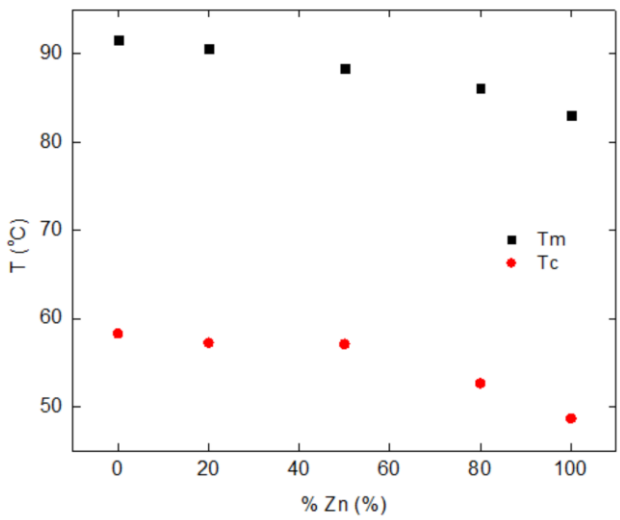

Figure 3.2 Melting and crystallization temperatures for all blend ratios of Blend 3 (see Table 2) that is blends of 3.8-Zn 60/1.5-Na 69. Squares (black) represents the melting temperature and circles (red) represent the crystallization temperature.

3.2 FTIR Analysis

FTIR spectroscopy provides an insight into the local ionic aggregate and bond structure changes that result from incorporating two different cations into EMAA ionomer blends.

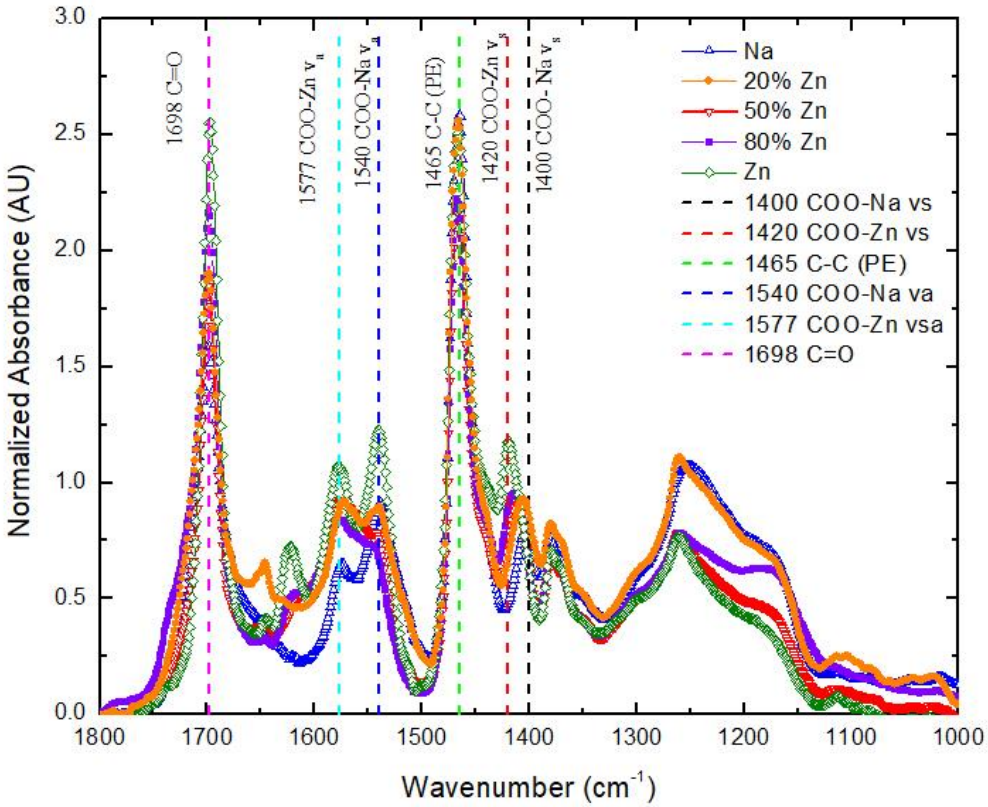

Figure 3.3 FTIR absorbance spectra of the blends of 3.8-Zn 60 and 1.5-Na 69 (blend 3). Vertical line labels v_a and v_s represent the asymmetric and symmetric stretching bands of the carbonyl bonding peak. Values on the y-axis are calculated using the equation: Absorbance=2-Log(% transmittance) and corrected for baseline shift and normalized with respect to film thickness and PE peak absorbance value (at 1465 cm^{-1}).

The FTIR peak at wavenumber 1698 cm^{-1} is attributed to the carboxylic acid dimer bond vibration[29] through the C=O double bond of MAA, which forms across the unneutralized acid groups. First, the 80%Zn/20%Na 1698cm^{-1} absorbance peak is broader and higher than the peaks at the other mixing ratios. The 80%Zn/20%Na blend has a higher C=O absorbance due to the higher MAA content of 3.8-Zn 60, increasing the number of MAA groups compared to 1.5-Na 69 with 1.5% MAA. The widening of the peak reflects hydrogen-bond interactions with the neighboring acids due to low counterion neutralization and the increased probability of hydrogen bonding. This agrees with the results obtained from DSC showing reduced cluster ordering increased clustering at 80% Zn/20% Na. Second, the region between the two COO^- asymmetric

peaks for neutralized ionomers at 1577 cm^{-1} for Zn and 1540 cm^{-1} for Na is indicative of structural changes in the local environment due to ionic aggregation. Tachino et al. [26] observed a new peak at 1565 cm^{-1} attributed to the formation of a conjugate binary metal salt of zinc acetate upon blending 50-75% Na with a Zn neutralized EMAA. Our results shown in Figure 3.3 are less clear due to the overlap of the asymmetric peaks. It can be seen, however, that the increase in absorbance around 1565 cm^{-1} seen for the 80%Zn/20%Na as a flat line between the two peaks of interest for the blends strongly suggests the presence of a new conjugate peak not present for the pure Zn or Na ionomers. This suggests the presence of an intermediate structure with an absorbance peak between the Zn and Na carbonyl peaks, and which matches the reported wavenumber and constitutive components of a zinc-sodium acetate conjugate metal salt. Furthermore, for the 20%Zn/80%Na blend, both asymmetric stretching bond vibrations for sodium and zinc with wavenumbers of 1540 cm^{-1} and 1577 cm^{-1} show higher absorbance values than the 50% and 80% blends, reflective of an increased number of bonds between the Na/Zn cations and the MAA groups. The 20%Zn/80%Na blend also shows a higher Zn asymmetric stretching peak compared to the 80%Zn/20%Na blend which has a higher Zn content, suggesting a larger fraction of Zn cations active as neutralizing counterions and as components of ionic clusters[70]. Finally, in agreement with previous studies[26,33], the symmetric COO^- peak for Na at 1400 cm^{-1} gradually shifts to that assigned for Zn at 1420 cm^{-1} with increasing Zn content. FTIR results show that the Zn component dominates the bond behavior due to its higher valency and ability to form stronger coordinate bonds. The higher asymmetric stretching band peaks also show that the 20%Zn/80%Na mixture has a high ratio of ionic aggregation, conjugation, and phase separation in agreement with the enhancement seen in DSC and in rheological and mechanical properties discussed below.

3.3 Linear Viscoelastic Behavior

As mentioned above, the rheological properties of the ionomers were determined using a rotational rheometer equipped with a cone-and-plate geometry. First, strain sweep experiments were performed to determine the limits of linear viscoelasticity at the angular frequency of 6.28 rad/s and the temperature of 140°C. Linear viscoelasticity has been observed within strain amplitudes of about 20% or less for all samples studied. Figure 3.4 presents the linear viscoelastic moduli for representative four out of the eight different blends. Measurements for all

tested blends are shown in the appendix. Two blends show synergistic effects/enhancement of viscoelastic moduli and complex viscosity (Figure 3.4 b,d- blends 3,7), and two blends are shown with no synergistic effects (Figure 3.4 a,c - blends 2, 4). For example, in Blend 3 (1.5-Na 69/3.8-Zn 60) the viscoelastic moduli of the blend with 20% Zn are higher than those of the pure components. In addition, terminal relaxation limit is not reached for the loss modulus (G" ~ ω^2) of blend 3 due to the rigid ionic cluster crosslinks leading to delayed dynamics. The continuous lines represent fits of the multi-mode Maxwell model:

$$G'(\omega) = \sum_{i=1}^{N} \frac{G_i(\omega\lambda_i)^2}{[1+(\omega\lambda_i)^2]} \tag{2a}$$

$$G''(\omega) = \sum_{i=1}^{N} \frac{G_i(\omega\lambda_i)}{[1+(\omega\lambda_i)^2]} \tag{2b}$$

where G_k are the relaxation strengths and λ_k are the relaxation times. The obtained parameters of λ_k and G_k found from the fitting are plotted in Figure 3.5 for each set of blend components.

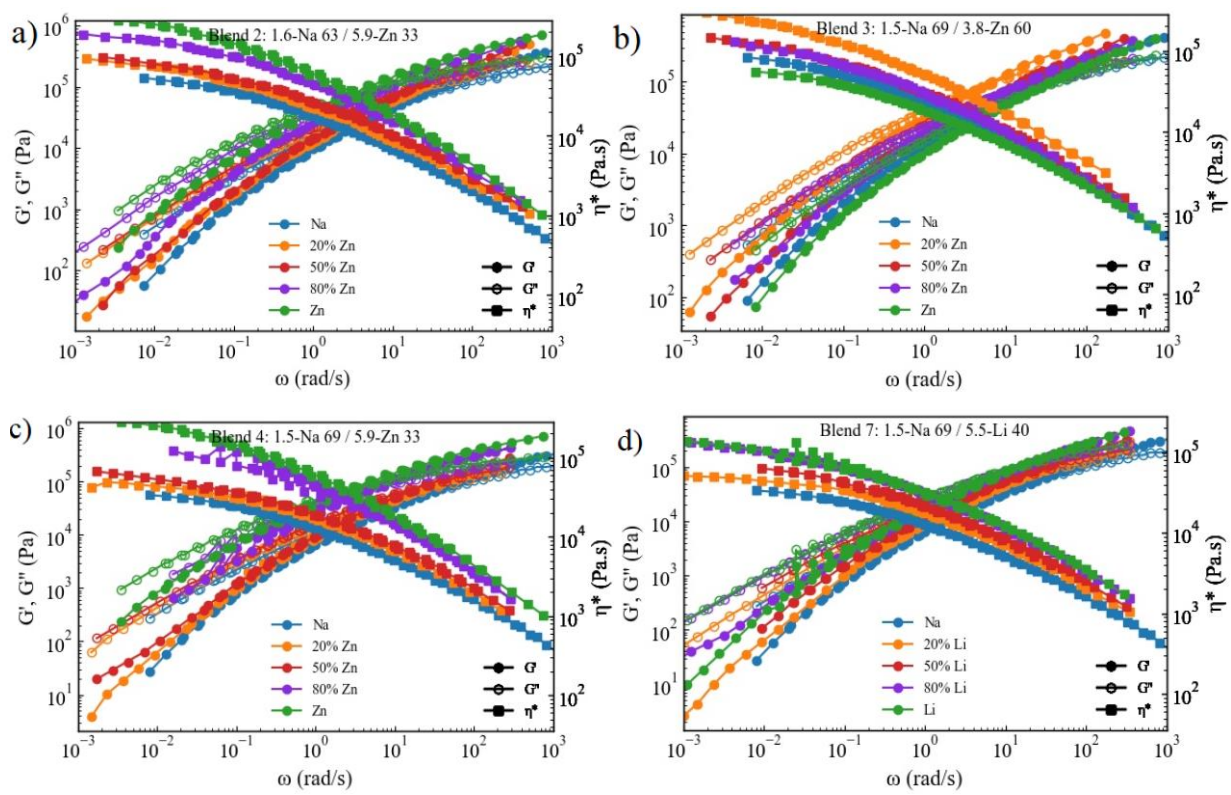

Figure 3.4 Linear viscoelasticity frequency sweep results for two blends showing synergistic effects/enhancement of viscoelastic moduli and complex viscosity (blends 3,7), and two blends showing no synergistic effects (blends 2, 4). Data are shifted to T_{ref} of 140ºC then fitted to a Maxwell model using 6 relaxation modes for the best-fit values. Continuous lines represent Maxwell fitting results.

Six relaxation times achieve the best fit rheological representation of the experimental data for all ionomers and their corresponding blends (plotted in Figure 3.4). The relaxation time distribution of ionomers compared to that of their blends is similar in shape, although is shifted to higher values of the relaxation modulus and higher values of relaxation time, when property enhancement is observed, such as in blend 3 at 20% Zn and blend 7 at 80% Li.

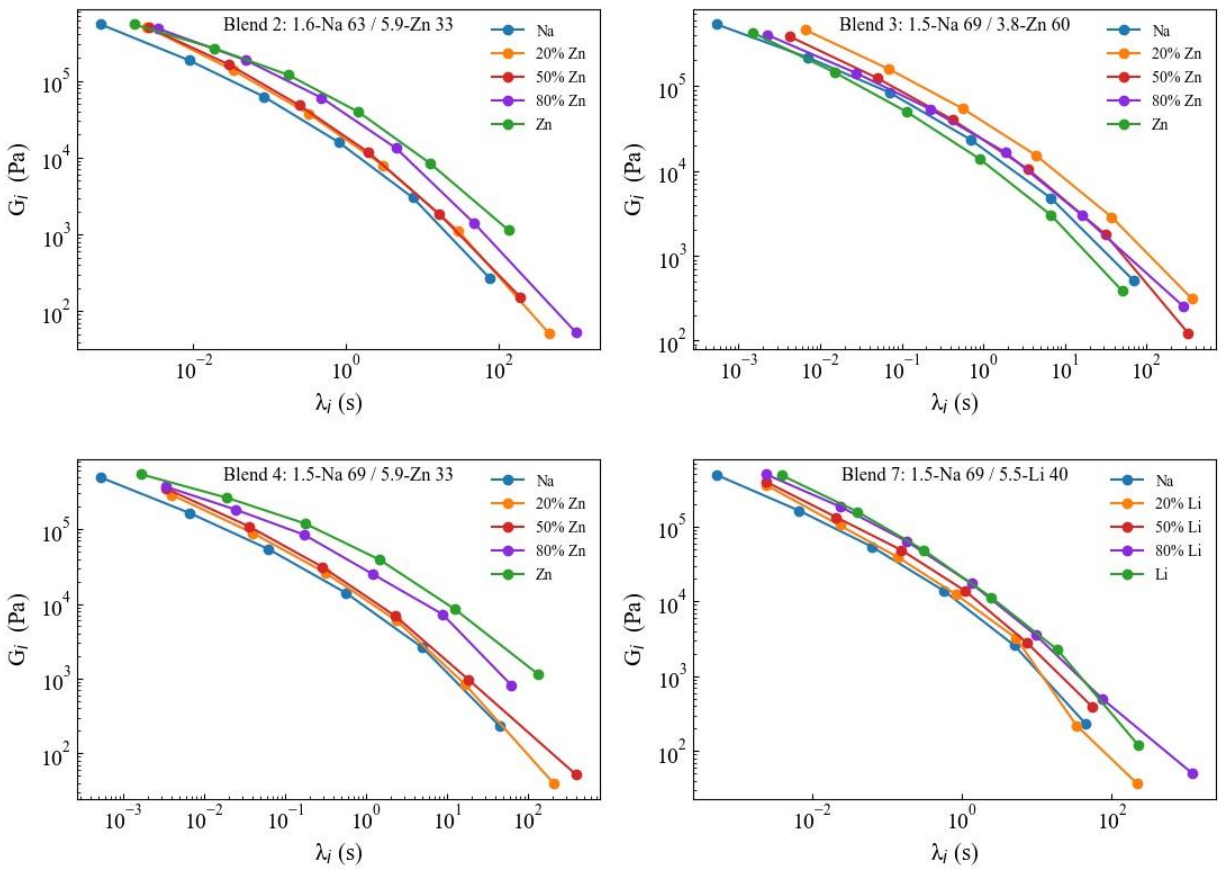

Figure 3.5 Maxwell relaxation spectra results for blends 3 and 7 showing increase in the relaxation strengths delay in relaxation at blend compositions exhibiting synergistic effects.

The zero-shear viscosity data can be used to show more clearly the synergistic effects. This can be calculated from the Maxwell relaxation times and strengths by $\eta_o = \sum_{i=1}^{N} G_i \lambda_i$. The zero-shear viscosity data are plotted in Figure 3.6 for various blends. More specifically, the zero-shear viscosity of the blend $\eta_{o,b}$ is plotted as a function of the ratio of the reference component, Zn for

blends containing Zn and Li for blends containing Li, with the balance being the other cation, sodium. Certain blends at specific compositions such 1.5-Na 69/3.8-Zn 60 and the 7.2-Na 65/ 5.5-Li 40 exhibit positive deviation from the log-additivity rule[71]:

$$\log \eta_{b,0} = \sum w_i \log \eta_{o,i} \quad (3)$$

where $\eta_{0,b}$ is the blend zero-shear viscosity and $\eta_{0,i}$ is the pure component zero-shear viscosity. Positive deviation from this rule represents immiscibility in the melt state, where in the present case can be interpreted as the presence of ionic aggregates phase-separated from the blend. This is in agreement with the DSC/FTIR results and also supports the enhancement in storage and loss moduli.

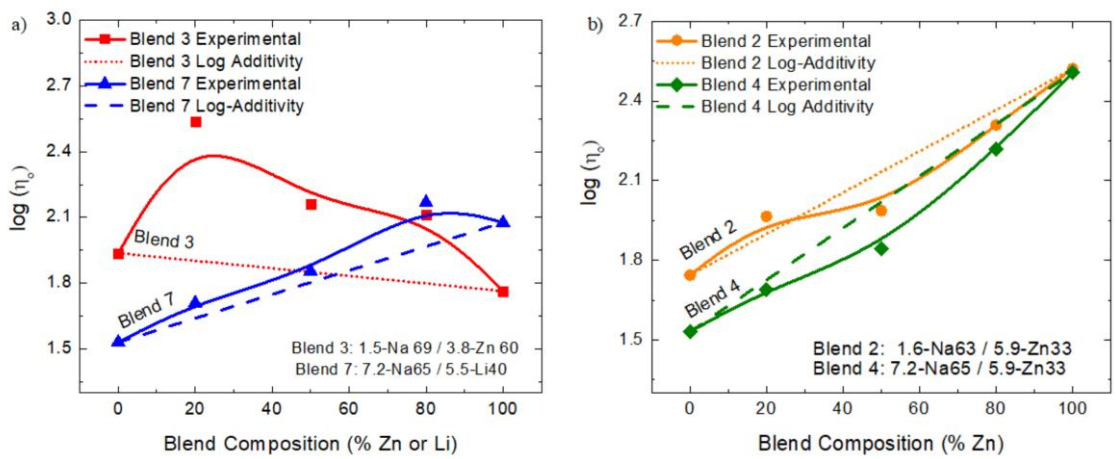

Figure 3.6 Log-additivity rule (dotted lines) and measured zero-shear viscosity for two blends showing positive deviation and thus synergistic effects (6a, blends 3, 7) and two blends showing negative deviation and thus no synergistic effects (6b, blends 2, 4). The continuous lines are based on the linear combination of the pure components and are drawn to guide the eye.

A four-fold increase in η_o is seen at 20%Zn composition for the Zn/Na blend (blend 3) and 1.6 times increase at 80%Li for the Li/Na blend (blend 7: 7.2-Na65/5.5-Li40). This η_o increase for blends 3 and 7 is also correlated with an increase in both relaxation modulus and relaxation time obtained from multi-mode Maxwell fitting of the master curve obtained from time-temperature superposition (tTS) shown in Figure 3.4 and Figure 3.5. Analysis based on the effect of ion charge and ion type shows that the higher ionic charge of Zn^{2+} is correlated well with more pronounced interaction compared to the single charge of Li^{+}. The enhancements in blend 3 (3.8-Zn 60/1.5-Na 69) of the four-fold increase in η_o are consistent with the proposed formation of large clusters of the conjugate sodium zinc acetate as explained by Tachino et al[26]. This is also confirmed by the decrease in the neutralized MAA groups due to the phase separation of the

counterions into clusters as revealed in the FTIR analysis. The largest enhancement seen at a Zn ratio of 20% also agrees with the required 33% Zn for the solvated zinc acetate conjugate salt[26]. For blend 7 (5.5-Li 40/ 7.2-Na 65) which shows 1.6 times increase in zero-shear viscosity, the enhancement is attributed to Li/Na aggregates which form more favorably in all tested lithium blends (blends 5-8) but with reduced intensity due to the reduced ionic strength and absence of coordination in Li^+/Na^+ ionomers compared to Zn^{2+}/Na^+.

However, a negative deviation in zero-shear viscosity of up to half of the value of linear mixing is observed for blend 2 (1.6-Na 63/5.9-Zn 33) and blend 4 (7.2-Na 65/5.9-Zn 33). The relaxation behavior of the larger molecular weight (MW) component, 5.9-Zn 33 in this case which has a MW twice as large, or a viscosity 6 times as large as that of the sodium component, masks any enhancement due to ionic aggregation that may be present in the sample. Therefore, these blends do not show synergism. It has also been observed that blends with a high un-neutralized MAA concentration do not show significant enhancement in rheological properties. High MAA content provides more bonding sites for ions along the polymer chain instead of being aggregated in clusters. This promotes ion hopping, where ions bound to MAA groups hop between ionic aggregates allowing for chain relaxation[18,37]. This can also be seen as a low level of neutralization which favors isolated cations instead of aggregate structures[15].

In addition to zero-shear viscosity, the activation energy (E_{act}) calculated using tTS shift factors shows a similar trend. Enhancement in E_{act} values for blends 3 at 20% Zn, 80% Na (3.8-Zn 60 / 1.5-Na 69) and blend 7 at 80%Li / 20% Na (5.5-Li 40/7.2-Na 65) is shown in Figure 3.7. The enhancement in E_{act} confirms the increased hindrance of flow and reinforced structure due to ionic cluster formation. In contrast, the E_{act} values for blends 2 (5.9-Zn 33, 1.6-Na 63) and 4 (5.9-Zn 33, 7.2-Na 65) decrease down to less than half of what the linear combination predicts, suggesting improved miscibility and softening of the crosslink structures due to the absence of reinforcing ionic aggregates. The large activation energy of the 5.9-Zn 33 component masks possible enhancement present in the system, revealing a state where interactions are not favorable. The high MAA content and low Zn counterion concentration in 5.9-Zn 33 do not favor phase segregation due to the large number of un-neutralized methacrylic acid groups in the system.

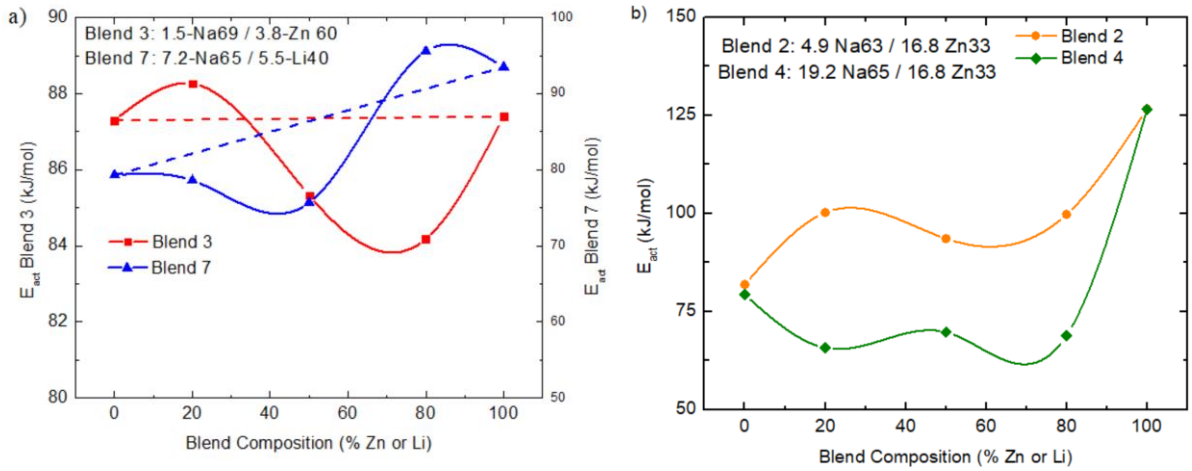

Figure 3.7 Activation energy values of pure components and binary blends at 20%, 50%, and 80% of the reference component (Zn or Li). Blends 3 and 7 show increased activation energy at the expected blend ratios of 20%Zn and 80% Li respectively. Blends 2 and 4 display a wide variation in activation energy values between those of the pure Zn and Na, not displaying significant synergism. The continuous lines are drawn to guide the eye.

A universal parameter combining the relevant molecular weights and neutralization is developed as a metric for determining favorable conditions for enhancement/synergism and correlate it with relative changes in rheological and mechanical properties for all blends. This single parameter will be useful as multiple variables vary widely across the tested materials (MW, MAA%, neutralization %, ion type, ion charge, ion size, and mixing ratio). A comparative study is performed to identify the parameters with the highest effect on the change in the rheological and mechanical properties. The parameter is referred to as the molecular weight-normalized neutralization and is calculated according to equation 4.

$$N_{MW} = \frac{100\ \mathrm{kg}/mol}{(x_1 MW_1 + x_2 MW_2)\ (MAA_{unneutralized\ 1\ 2})} \tag{4}$$

where 100 is a scaling factor in the numerator, x_1 and x_2 are the mass fractions of components 1 and 2 of the binary blend, MW_1 and MW_2 are the molecular weights in kg/mol of components 1 and 2, and $MAA_{unneutralized}$ is the total unneutralized mole percent of methacrylic acid calculated by subtracting the total MAA content by the neutralized mole percent of both components. Small values of N_{MW} correspond to low neutralization and high total MW, while high N_{MW} implies high neutralization and small MW of the two pure ionomers. It is noted that the N_{MW} depends only on the molecular weight characteristics of the two parent ionomers and does not require additional rheological testing. This metric, N_{MW}, is correlated with enhancement in

zero shear viscosity, calculated as the ratio of zero-shear viscosity of the blend to the zero-shear viscosity according to equation 4 by a linear combination of the zero-shear viscosities of the two pure ionomers.

$$\eta_o \; Relative \; Increase = \frac{Experimentally \; measured \; \eta_o}{x_1\eta_{o,\;\; component\;1} + x_2\eta_{o,\;\; component\;2}} \qquad (5)$$

Figure 3.8 shows the zero-shear viscosity enhancement (Equation 4) as a function of the MW-normalized neutralization, N_{MW}. The dashed line separates the points showing the enhancement (>1). Overall, a reasonable correlation exists where the zero-shear viscosity enhancement increases with N_{MW}. Low values of MW-normalized neutralization are associated with no enhancement of zero-shear viscosity (values below 1) indicating negative deviation from the linear additivity rule (e.g. blends 2, 4). On the other hand, binary blend components with high neutralization and lower MW such as blends 3 and 6 show larger increases in zero-shear viscosity (positive deviation from the linear additivity rule). The independence of the type of ion (valency) agrees with findings in literature about a high dependence on the degree of ionization, and no dependence on the type of ion[13].

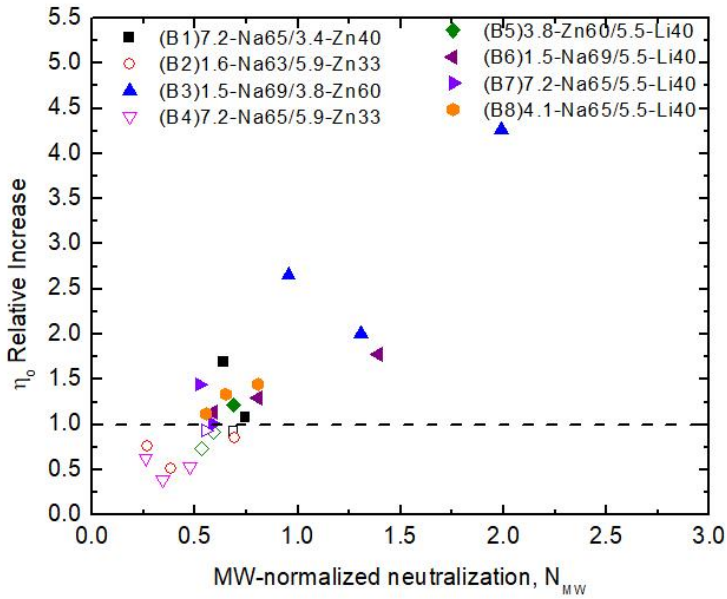

Figure 3.8 Relative increase compared to the linear combination value of zero-shear viscosity at 140°C for blends 1 through 8 plotted against MW-normalized neutralization. Legend labels are the blend number followed by the composition of the two pure ionomer components. Open symbols represent binary mixtures with a relative decrease in η_o, and filled symbols represent relatively increased η_o values with respect to the linear combination.

Besides viscosity, the dynamics of the relaxation mechanisms also give insight into the molecular structure of the ionomer blends. To investigate the timescales of the ionic associations versus chain relaxation, we have implemented the scaling laws of the theory of reversible associations developed by Leibler et al[30] explained for EMAA ionomers by Tomkovic et al.[29], to calculate the lifetime of associations, τ_s. The association lifetimes for each sample is calculated using the relationship $\tau_s = \tau_{rep}/Z_E Z_S^2$ where τ_s is the association lifetime, and τ_{rep} is the reptation time set to be equal the longest relaxation time obtained through Maxwell relaxation fitting (Equations 1a,b), which yields values close to those of the inverse frequency at the G' and G'' crossover. Z_E is the number of entanglements ($Z_E = M_w/M_e$) with M_w as the molecular weight and M_e the entanglement molecular weight equal to 1200 g/mol[29]. Z_S is the average number of associations per chain. Values of τ_s are calculated to be within the range of 10^{-4} to 10^{-2} as reported in literature[29]. The results plotted in Figure 3.9 show a correlation between the association lifetime and N_{MW}. It is notable that the blends which show enhancement in zero-shear viscosity (Figure 3.8) also exhibit a higher average association lifetime as shown in Figure 3.9a. From these values and from results published by Register et al[18], we can confirm that ionic clusters with high neutralization form a stable ionic crosslink structure which remains in its associated form for longer durations (Figure 3.9 b). This prevents relaxation of the EMAA backbone, increasing the modulus and viscosity values and delaying terminal relaxation through a prolonged lifetime of associations. Table 3.1 shows the scaling analysis timescales for blend 3 with significant blend interaction. It is notable that the Zn/Na ratio of 0.55 for the 20%Zn blend agrees with the reported range of 0.5-0.75 for the formation of Zn/Na acetate conjugate salt[26].

Table 3.1 Sample calculations using the sticky reptation scaling analysis for the blend composed of 1.5-Na69/3.8-Zn60. The largest increase in viscosity is correlated with the longest lifetime of association, sticky Rouse time, and reptation time

Blend Components	Mixing Ratio	Mw (kg/mol)	mol% MAA	Neutralization %	Neutralized MAA mol %	Zn/Na mol% ratio	Z_S	Z_E	τ_e SR time (s)	τ_s association time (s)	τ_{rep} (s)	η_o (kPa.s)
1.5-Na 69	0	73	1.5	69	1.04	0	9	60	3.1×10^{-4}	1.5×10^{-2}	69	86
Na/Zn 80/20%	0.2	74	2.0	67.2	1.28	0.55	11	62	1.5×10^{-3}	4.4×10^{-2}	359	344
Na/Zn 50/50%	0.5	77	2.7	64.5	1.66	2.20	15	64	1.2×10^{-3}	2.1×10^{-2}	324	144
Na/Zn 20/80%	0.8	80	3.3	61.8	2.03	8.81	19	67	9.3×10^{-4}	1.1×10^{-2}	278	170
3.8-Zn 60	1	82	3.8	60	2.28	1	22	68	1.5×10^{-4}	1.5×10^{-3}	50	58

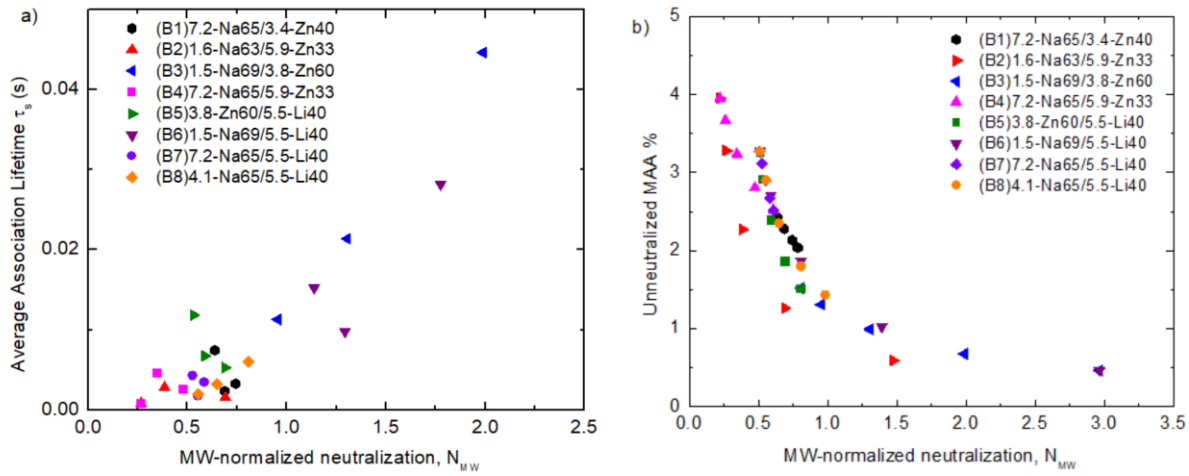

Figure 3.9 (a) Molecular weight normalized neutralization vs average association lifetime. (b) Molecular weight normalized neutralization vs degree of unneutralized MAA (mol %). The strong inverse relationship describes the controlling parameter as the degree of neutralization/unneutralization, and a secondary effect of MW in equation 3 which magnifies or diminishes the presence of enhancement.

3.3.1 Error Analysis of Linear Viscoelastic Experiments

To verify the accuracy and reproducibility of the above measurements, multiple experimental controls were tested to ensure that sample preparation did not alter any material properties.

1. To control for time-dependent aggregate formation and degradation during rheological testing, a sample of blend 2 (80%Zn/20%Na) is subjected to a time sweep experiment over the duration of 1 h at 5% strain and 1 rad/s frequency at 140ºC. Variation in storage modulus, loss modulus, and complex viscosity is within 5%, showing no significant temporal dependence over the duration of SAOS experiments.

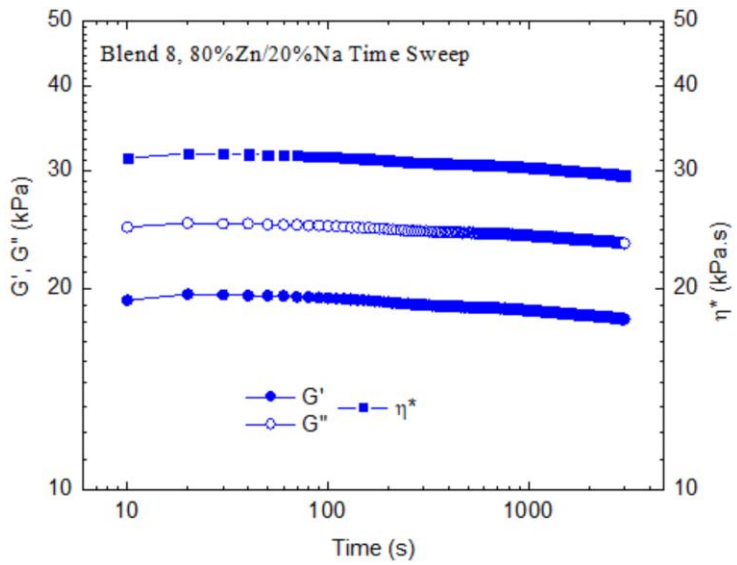

Figure 3.10 Time sweep results for blend 8 at 80%Zn/20%Na showing minimal change in linear rheological properties over the duration of the experiment.

2. To control for variability across measurements and anisotropy across a disk, different samples from a pure zinc ionomer disk were tested using small-strain oscillatory shear (SAOS). Reproducibility is confirmed as the frequency sweep curves overlap, and viscosity values agree to within 4%. Duplicate testing of subsequent blends is not performed for each disk since the samples are confirmed to be homogeneous and stable over time with highly reproducible results.

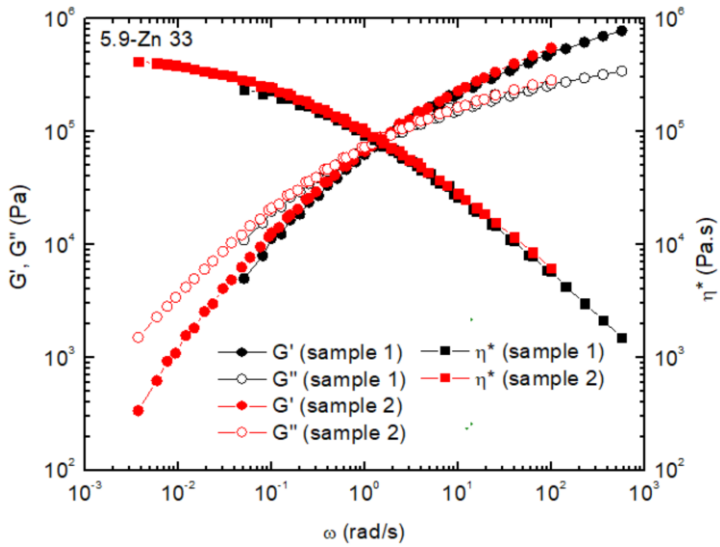

Figure 3.11 Mastercurve at 140°C of SAOS testing of two samples from the same disk of a 5.9-Zn 33 ionomer.

3. To control for solvent effects, two 5.9-Zn 33 samples were tested. The first sample was prepared through compression molding and dried for one week. The second sample was prepared by dissolving the zinc pellets using the binary blend preparation process, followed by rinsing, drying, and compression molding. No significant deviation was observed in the SAOS curves. This confirms that solution mixing as a blend preparation process does not significantly alter the properties of the ionomers.

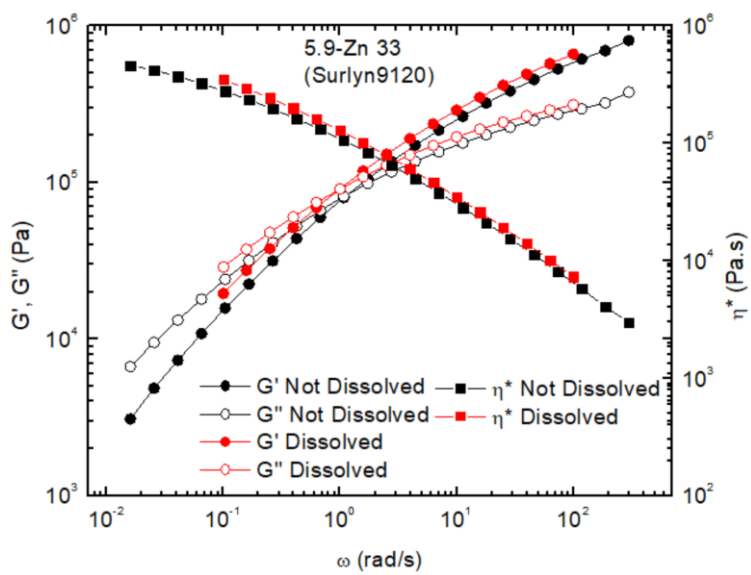

Figure 3.12 SAOS results at 140°C for 5.9-Zn33 samples prepared through compression molding (Not Dissolved) or using the solution mixing procedure used to prepare binary ionomer blends (Dissolved) followed by compression molding.

4. To control for blend preparation variability, two batches of blend 2 (5.9-Zn 33 / 1.6-Na 63) at 50%Zn/50%Na mixing ratio were prepared using the same procedure described in the previous chapter. SAOS results from the two batches agree to within 6%. This shows that the blend preparation process is repeatable.

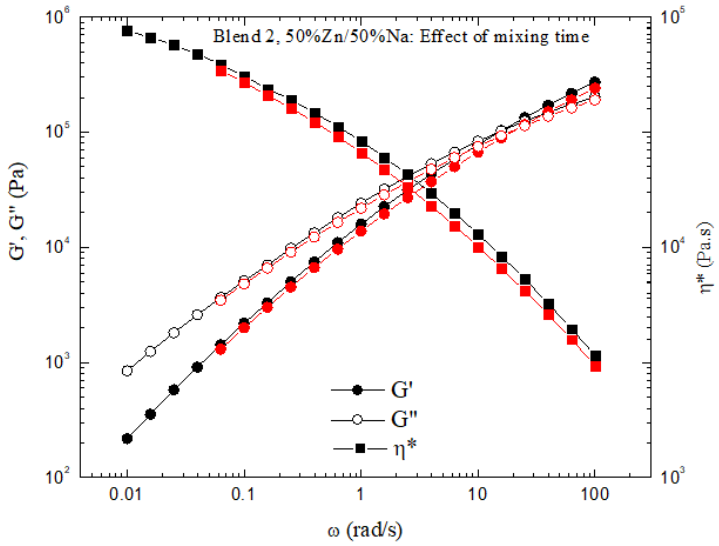

Figure 3.13 Frequency sweep results for blend 2 at 50%Zn/50%Na composition dissolved for different durations during solution mixing. Different colors correspond to different samples.

In summary, linear viscoelastic testing of ionomer blends neutralized by different cations exhibit enhanced rheological properties and prolonged ionic association time compared to the pure component ionomers for blends with low combined molecular weight and high extent of neutralization.

3.4 Nonlinear Viscoelasticity

3.4.1 Stress Relaxation

To investigate the effect of larger, nonlinear deformation on the presence of synergy in the melt state, stress relaxation experiments are performed which span a range of strain amplitudes up to 1000%. The results for blends 2, 3, 4, and 7 are presented in Figure 3.14.

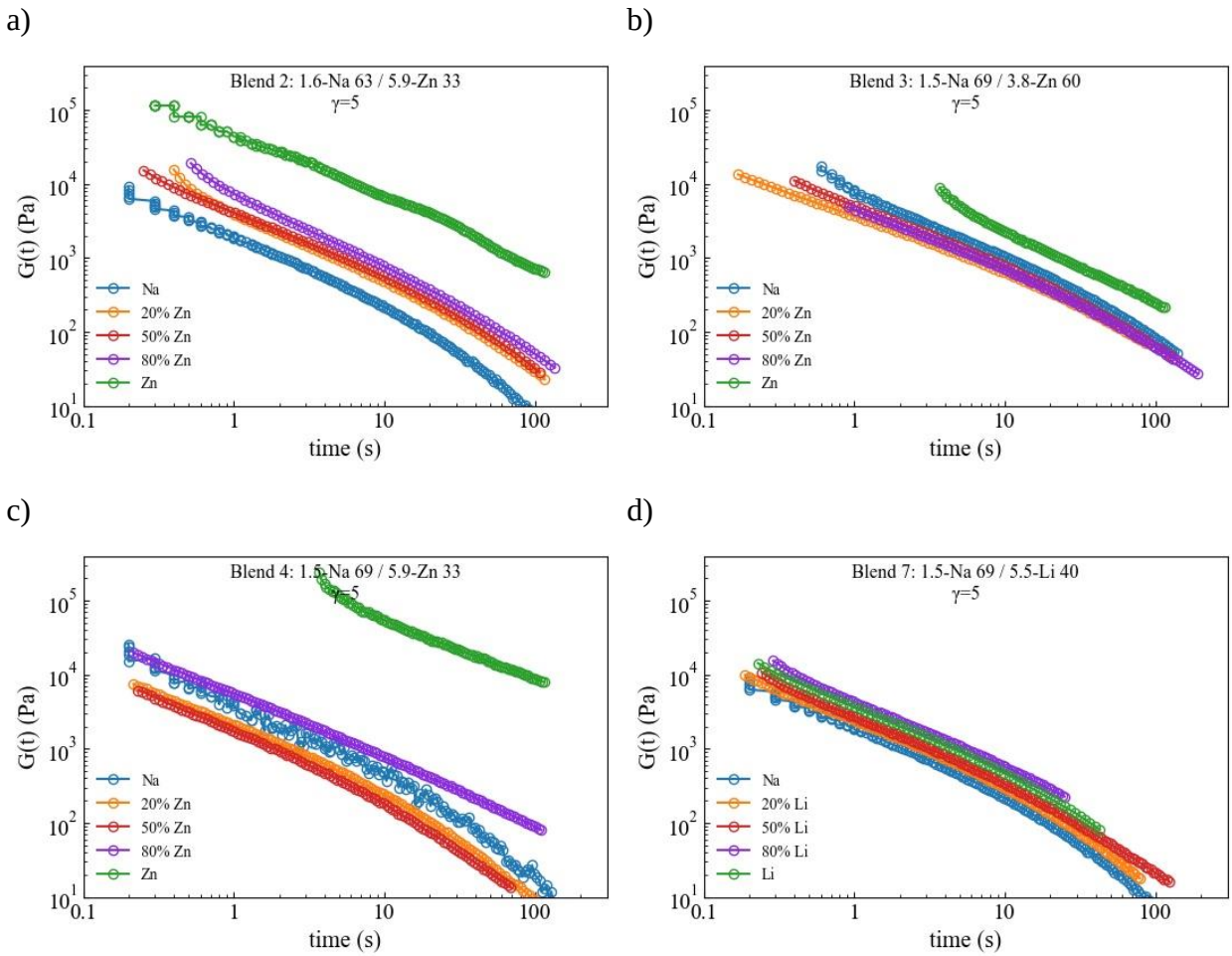

Figure 3.14 Nonlinear strain relaxation modulus vs time at a strain amplitude of 5 (500%) for Blends 2 and 4 (no synergistic effects) and blends 3 and 7 (with synergistic effects).

The stress relaxation curves at various strains were used to obtain the damping functions of all blends at all compositions. The damping coefficient of the four discussed blends (2, 3, 4, 7) are presented in Figure 3.15. The damping function of blend 3 at 20%Zn maintains the highest value of damping coefficient (Figure 3.15 b). Comparing the results from Figure 3.14 and Figure 3.15 shows that blends of strongly interacting cations maintain a high damping coefficient over high strain rates, suggestive of a crosslinked structure reinforcing a solid-like material. The maintained high damping coefficient and high relaxation moduli are attributed to strongly crosslinked ionic aggregates which separate from the EMAA chains and can store elastic energy, reducing the modulus but reinforcing the network structure and resisting deformation due to strong electrostatic and polar forces (less damping due to delayed/hindered relaxation).

However, non-interacting blends show a higher drop in relaxation modulus at high strain rates reflective of soft viscous polymers with no physical crosslinks. For example, blends 2 and 4 have relaxation moduli with intermediate values which quickly decrease in magnitude at higher strain values similar to non-ionomeric polymer melts.

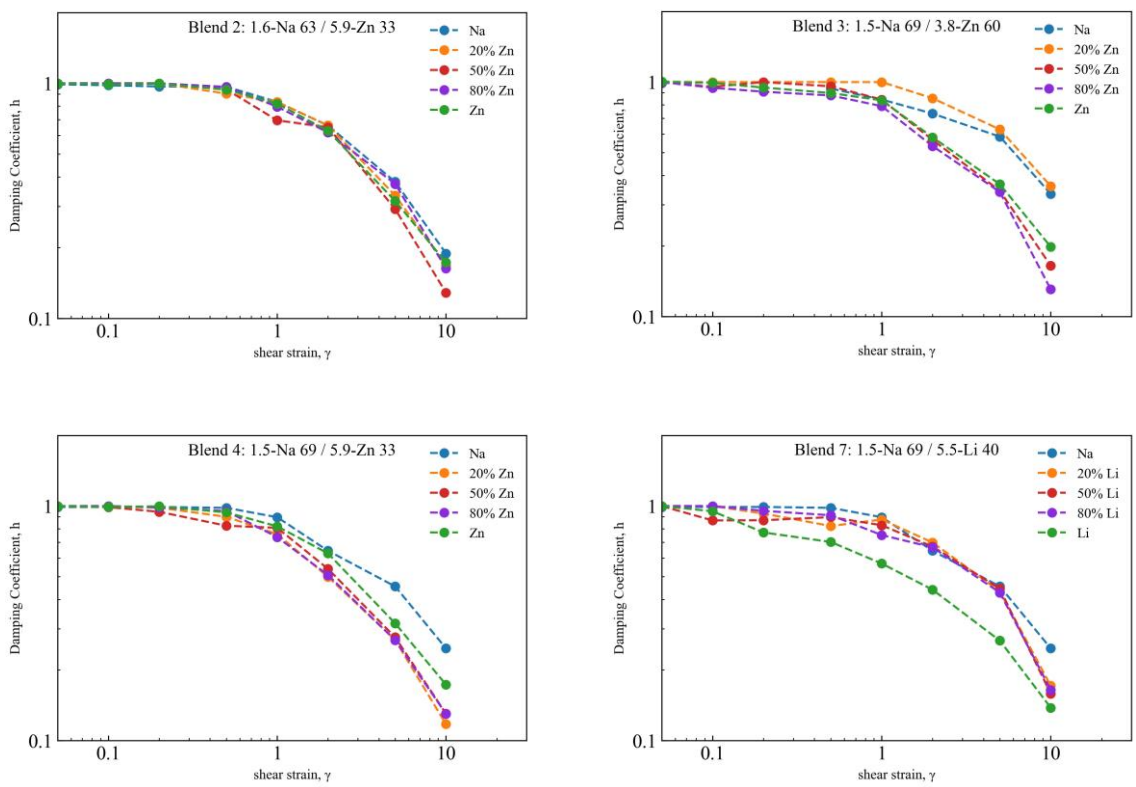

Figure 3.15 Damping function of various blends. For blend 2, damping coefficient decreases with neutralization reflective of strain softening due to ionic clustering at the high Zn contents required for aggregation. For blend 3, 20% Zn has the highest damping coefficient values, representative of the maintenance of a constant relaxation modulus due to a stabilized internal structure by the ionic aggregates.

3.5 Uniaxial Extensional Properties

An additional investigation of nonlinear deformations is through uniaxial extension tests in the melt state. Uniaxial extension tests were performed at 140°C at Hencky strain rates of 0.5, 2, and 5 1/s for all samples. The results are shown in Figure 3.16. Strong stain hardening effects are obtained for all components and blends due to the presence of ionic associations/clusters. These results are normalized by 3 times the linear viscoelastic envelope ($3\eta^{+}$) to obtain the strain hardening factor (SHF) shown in Figure 3.17. Blend 3 at 20%Zn and blend 7 at 80% Li previously shown to exhibit enhanced rheological properties in the linear viscoelastic region

show no sign of synergism (increase of strain hardening) at high strain rates. Blends 2 and 4 with no significant rheological enhancement show an increase in extensional viscosity with increasing strain rate only in accordance with the linear combination of their component ionomers. The absence of observed synergism in these nonlinear viscoelastic tests is due to the high strains imposed on the polymer chains in the melt state. It has been shown that higher shear rates/strains along with chain mobility at the high temperatures in the polymer melt state can readily detach polymer chains from the ionic core to dissipate the additional force load, resulting in a measured increase in mechanical properties[72]. This disrupts the mechanical enhancement created by ionic crosslinks and clusters and eliminates the reinforcing effect of synergism.

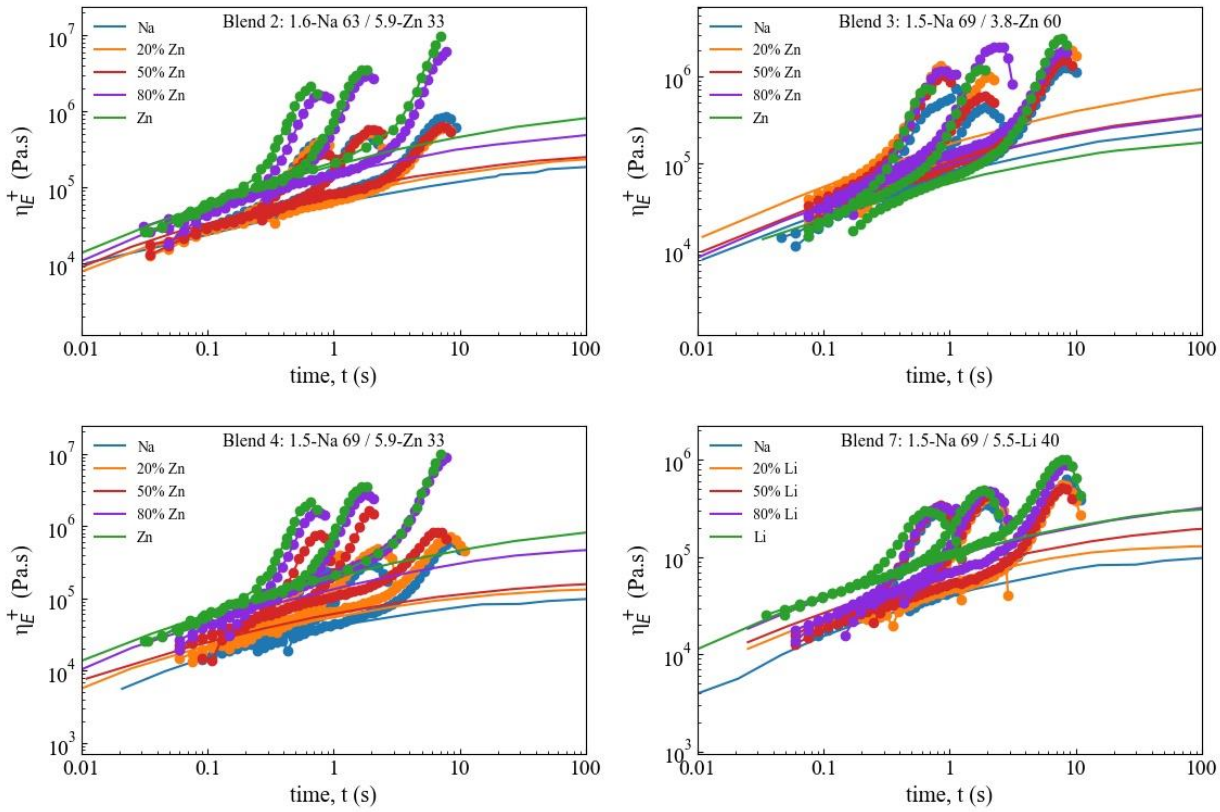

Figure 3.16 Extensional viscosity and the corresponding linear viscoelastic envelope for blends 2,3,4 and 7 tested at 140°C.

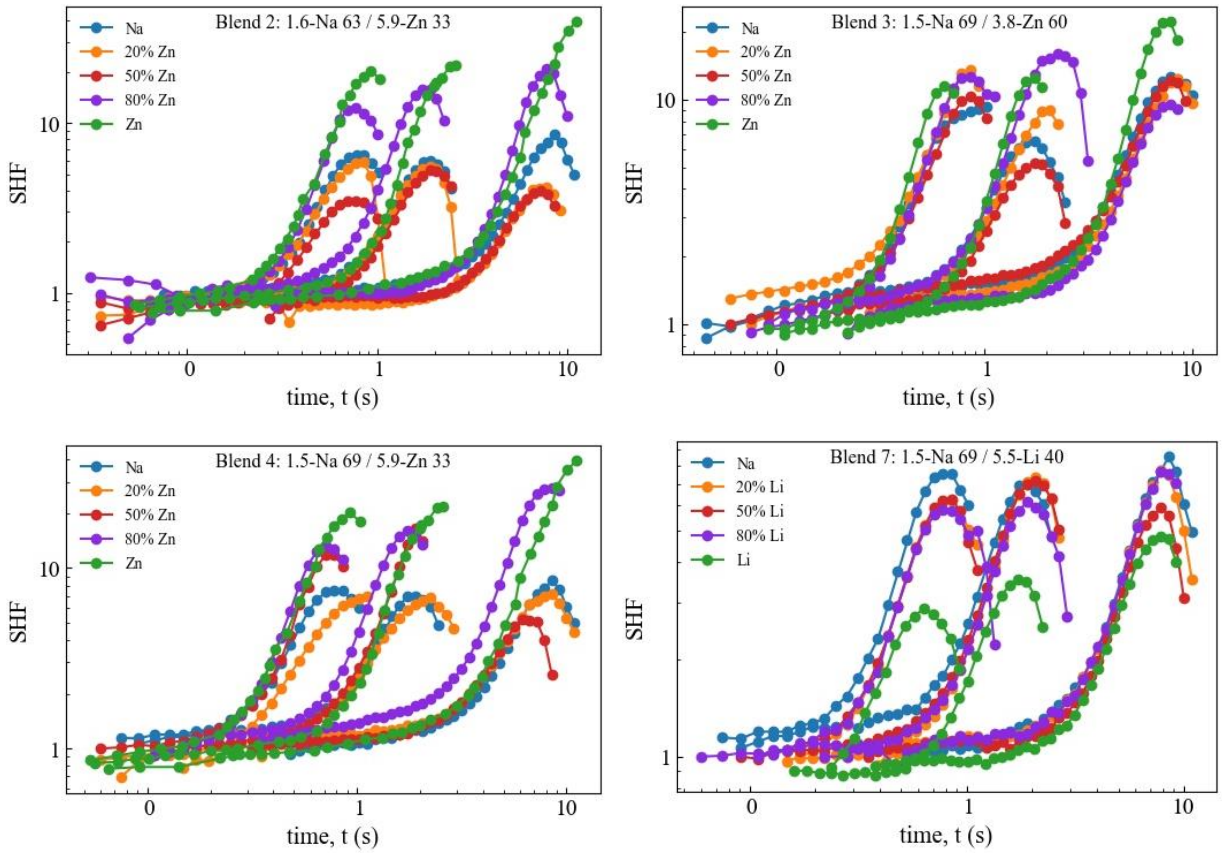

Figure 3.17 Strain Hardening Factor (SHF) from the uniaxial extensional viscosity data tested at 140°C (Figure 3.16) for two interacting blends (Blends 2 and 4) and two non-enhanced blends (Blends 3 and 7).

3.6 Mechanical Properties

To investigate the effect of ionic clusters in an ordered state and eliminating the possibility of their dissipation at high temperature, the solid-state tensile properties are tested to extract the Young modulus (E), yield stress, yield strain, and stress at 100% strain at 75°C. A temperature between the crystallization temperature and the melting temperature was chosen to maintain the polymer in the solid state yet allow its deformation upon stretching. Young's modulus, *E*, is the initial linear slope of the stress versus strain curve calculated as the slope of the linear fit through strain values up to 10% during the initial tensile elongation. Young's modulus presented in Figure 3.18 shows a positive deviation for blends 3 and 7 which exhibit synergism in melt state rheology[18]. A maximum *E* value of 22MPa at the 20%Zn ratio of blend 3 is 34% above the linear mixing value. This demonstrates the enhanced rigidity of the combination of 1.5-Na 69 and 3.8-Zn 60. The effects for blend 7 are less pronounced. Furthermore, analysis of the yield stress and the stress at 100% strain shown in Figure 3.19 support the increase in strength and reduction in

deformability. The yield point is calculated as the stress at the end of the initial linear or elastic increase in the stress-strain curve, also as the onset of the decrease in the derivative of stress with respect to strain. The yield stress of blends 3 and 7 increases for the binary blends compared to the pure components suggesting an increased rigidity and sustained elastic region before necking due to the physical crosslinks. It has also been shown that the size of ionic clusters which dictates the mechanical properties increases with neutralization[70], and this is further enhanced for the conjugate zinc-sodium salt formed through binary blends. The simultaneous decrease in yield strain for blend 3 agrees with the expected decrease in elongation along with the increase in strength.

On the other hand, blends 2 and 4 consisting of 5.9-Zn 33 with a high MAA content and a low neutralization degree show a negative deviation in E, yield stress, and stress at 100% strain. This is also shown for blend 3 at the 80%Zn ratio which was shown to have increased neutralization of the methacrylic acid groups instead of phase segregation through FTIR analysis. The reduction in mechanical strength as well as in the rheological properties and increased softening during stress relaxation support the plasticizing effect of the MAA chains solvating the available counterions, and not the formation of ionic clusters as crosslinks.

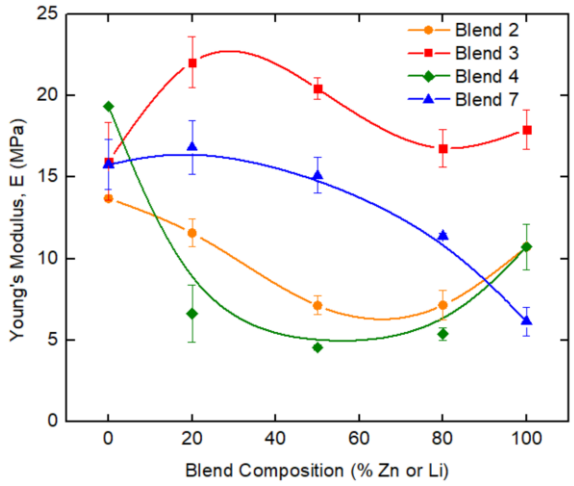

Figure 3.18. Young's modulus values at 75°C of the blends discussed showing increased Young's modulus values for blends 3 and 7 beyond the linear combination. Blends 2 and 4 show a strong negative deviation in Young's modulus upon mixing. These results agree with linear rheological measurements as well as DSC/FTIR results.

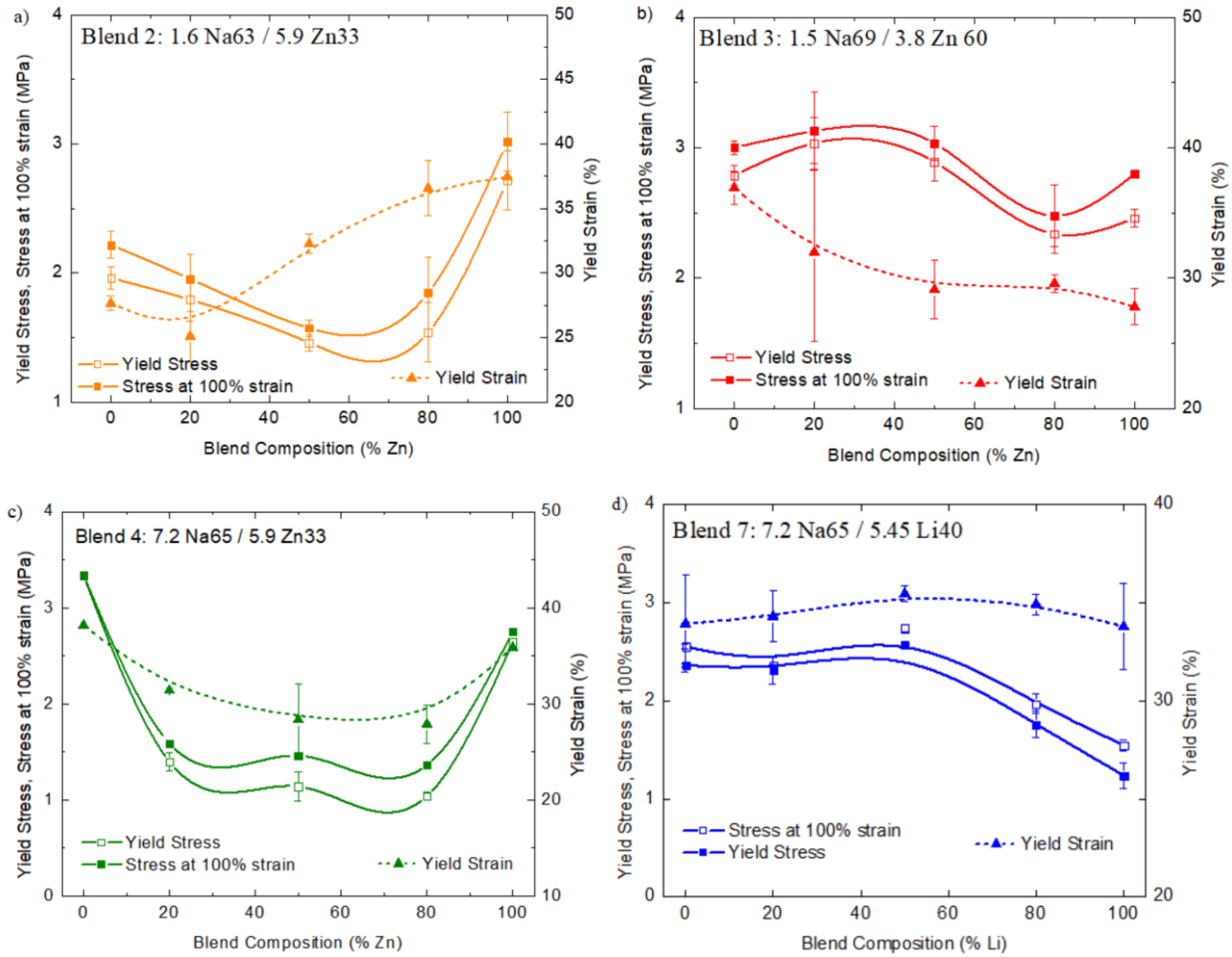

Figure 3.19. Yield stress, yield strain, and stress at 100% strain for 4 different binary blends. Positive deviations suggest reinforcement by ionic multiplets and clusters which act as crosslinks (Blends 3 and 7). Negative deviations suggest increased miscibility and softening due to increased chain motion by ion hopping and neutralization (Blends 2 and 4).

Similar to the analysis performed for the enhancement of the zero-shear viscosity, the enhancement in Young modulus (Young modulus of blend normalized by the Young modulus based on the linear combination of the Young moduli of the individual components) is correlated with the universal parameter "Molecular weight-normalized neutralization", N_{MW}. The Young's modulus of all eight combinations with the 3 mixing ratios each (20%, 50%, and 80%) are plotted in Figure 3.20. The significant metric for solid-state enhancement is the same as that for linear rheology, which is proportional to the difference in the molecular weight of the two pure ionomers and to the inverse of the unneutralized MAA content. Values on the lower end of the x-axis correspond to blends with a large combined MW and to a low level of neutralized MAA content. These values are correlated with a lower value of E compared to the linear combination

expected value. For instance, blend 4 composed of two ionomers with MW 114,200 g/mol and 114,500 g/mol with the smallest difference between the two (ΔMW = 300g/mol) shows the smallest increase in the Young's modulus. The upper end of the x-axis with blends of similarly sized ionomers and high degrees of neutralization shows larger increases in *E* suggesting these two factors to contribute to interaction due to ionic aggregates.

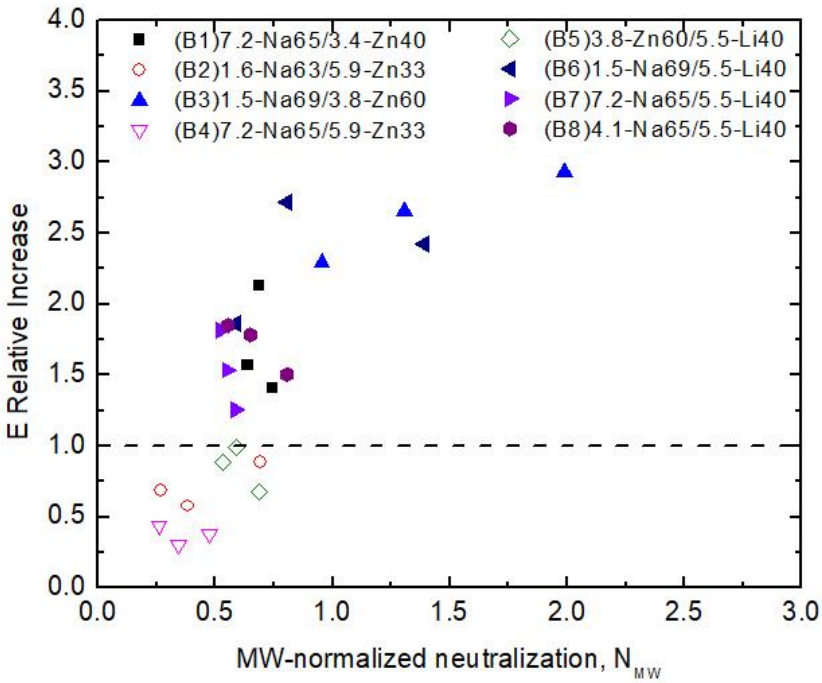

Figure 3.20 Relative increase in Young's modulus measured at 75°C for 20%, 50%, and 80% binary mixtures for blends 1 through 8 plotted against MW-normalized neutralization. Open symbols represent binary mixtures with a relative decrease in Young's modulus, and filled symbols represent relatively increased E values with respect to the linear combination

To summarize the impact of binary cation blends on the linear and nonlinear viscoelastic properties, Table 3.2 lists all 8 blends and a binary (+/-) indicator on the presence (+) or absence (-) of overall synergism for each property for each blend. The presence of interactions is determined by comparing the experimentally measured values relative to the linearly combined values of the two constituent ionomers. Synergism is observed in blends with low MAA content of the pure ionomers, high ionic neutralization, and high MW of the EMAA chains. When present, interaction is stronger for Zn/Na blends compared to Zn/Li or Na/Li binary blends. Using the analysis in this study, the selection of ionomer components can determine if the binary mixture rheological and mechanical properties will exceed those of the pure components.

Table 3.2 Summary of presence vs absence of synergism for each blend under melt state testing: linear viscoelasticity (LVE) (η_o, τ_s), Non-LVE (stress relaxation, damping coefficient), and solid state testing in tensile mode (Young modulus, yield stress, yield strain).

Blend #	Blend Components	N_{MW}	η_o	τ_s	Non-LVE	Solid-state (tensile)
1	7.2-Na 65 / 3.4-Zn 40	+	+	-	+	+
2	1.6-Na 63/ 5.9-Zn33	-	-	-	-	-
3	1.5-Na 69 / 3.8-Zn 60	+	+	+	+	+
4	7.2-Na 65 / 5.9-Zn 33	-	-	-	-	-
5	3.8-Zn 60 / 5.5-Li 40	-	-	-	+	-
6	1.5-Na 69 / 5.5-Li 40	+	+	+	+	+
7	7.2-Na 65 / 5.5-Li 40	+	+	-	+	+
8	4.1-Na 65 / 5.5-Li 40	+	+	-	-	+

Chapter 4: Conclusions and Recommendation

This chapter summarizes all findings and provides recommendations for future work. Possible applications based on the discussed binary EMAA ionomer blend behaviors are also proposed.

4.1 Conclusions

A rheological and mechanical study of binary blends of cations neutralizing EMAA ionomers is presented with a focus on the molecular and processing conditions that favor synergistic interactions within ionic aggregates. Rheological (shear and extensional) and tensile mechanical testing of EMAA ionomers with binary blends of Zn, Na, and Li neutralizing cations in the melt and solid state reveals enhancement in properties for certain combinations beyond what is obtained from the linear mixing of the corresponding properties of their pure components. It has been found that high ion neutralization content along with low MW and high valency are most likely to lead to strong synergistic ionic interactions in ionic clusters since these conditions favor phase segregation and stable crosslink formation.

Linear viscoelastic testing and Maxwell relaxation spectrum analysis reveal an increase in the linear region relaxation modulus, relaxation time, and zero-shear viscosity. The property enhancement has been captured in the definition of a universal parameter, the "Molecular weight-normalized Neutralization" (N_{MW}) applicable to all tested binary blends, composed by the inverse of molecular weight and neutralization. N_{MW} is found to be proportional to the degree of synergism, identified through rheological and mechanical results such as relative increases in zero-shear viscosity, average association lifetime, and Young's Modulus. High neutralization with lower-sized chains is correlated with higher extents of synergism. Tested blends with either Zn/Na or Li/Na mixtures are found to exhibit enhanced properties. If synergy is present, its significance is higher for binary blends containing zinc counterions due to the high valency of their ionic charge and their coordinate bond formation with multiple carboxylic acid groups. The highest degree of enhancement in rheological and mechanical properties is seen for the 1.5-Na 69/ 3.8-Zn 60 blend which has the lowest combined MAA content across all tested blends.

Results of FTIR spectroscopy support the conditions found for enhancement at low methacrylic acid content and high ion neutralization. However, a high MAA content acts as a plasticizer and as such holds ionic counterions from aggregating into multiplets or further into clusters. The

plasticizing effect is seen as a decrease in viscosity and mechanical properties and accelerated chain mobility, rapid relaxation, and strain softening. Nonlinear extensional testing and stress relaxation cause internal restructuring and disruption of the ionic aggregates leading to minimal synergistic effects. Therefore, stresses applied well beyond their linear viscoelastic region do not promote sustained aggregation and synergistic behavior in the melt state. Other factors that disrupt ionic interactions is the presence of high valency ions such as Zn^{2+} on high molecular weight chains which dominate chain relaxation dynamics through extensive coordinate bond formation which can mask blend properties.

Tensile testing in the soft solid state reveals similar results to the melt state concerning the conditions and blend ratios that favor enhancement due to ionic clusters of dissimilar cations. However, binary ion blends with high ion content alone does not promote interaction. Ionomer blends formed by selecting similar, low molecular weights for the two components, different valency of ion types, low MAA content, and high ion concentration can yield a material with significantly enhanced rheological and mechanical properties compared to its constituent components.

4.2 Recommendations

The findings of this study present a variety of mechanisms and dynamics that occur in binary cation neutralized EMAA blends. To cover the full spectrum of molecular weights and degrees of neutralization which would verify the developed universal parameter – molecular weight normalized neutralization N_{MW}, multiple intermediate experiments can be conducted. First, the effect of transition metal cations and valency on the strength of the bonds in aggregates can be investigated by comparing calcium or magnesium ions to the tested zinc ions which have shown to dominate rheological and mechanical properties of the resulting materials. Non-transition metals unable to form coordinate bonds, even with higher valency, might not result in the same synergistic effects as zinc has shown. Concerning the effect of ion type on the degree of interaction, Zn/Na combinations have shown the largest magnitude in increase. This increase is favored by the low MAA content present in the pure EMAA components (1.5-Na69, 3.8-Zn 60). The distinction in the effect of ion type has not been clearly identified due to the high MAA content present in the lithium ionomer (5.5 mol%). It is of interest to form a blend with a

comparable low MAA content (eg 1.5-Li 69) to determine the extent of interaction in both Na/Zn or Li/Zn blends. A similar argument can be made for the Na/Li blends to investigate ionic synergism at low MAA content or high degrees of neutralization.

Second, gradual degrees of neutralization of Zn and Na can be tested by controlled addition of counterions to unneutralized copolymer EMAA chains, which would provide a systematic overview of desired N_{MW} values that equally cover the experimental range. Third, and having the information about the acid and ion concentrations for increased rheological and mechanical properties, localized optimization of the mixing ratios of the blends (i.e refined between 0, 20%, 50%, 80%, or 100%) can provide the blend with the global maximum of the rheological or mechanical property. This study can inform the production of customized ionomeric materials for a wide range of industrial or commercial applications.

Finally, refined investigation into molecular structure through X-ray absorption (XAS) can provide information on the distribution of cations inside ionic aggregates and can support the findings of rheological studies. In addition, inductively-coupled plasma mass spectrometry (ICP-MS) can identify the ratio of neutralizing cations as well as PE backbone chain carbon and hydrogen atoms giving a quantitative metric to investigate aggregate composition. This will also allow the optimization of the cation ratio of Zn/Na, Li/Na, or Zn/Li which will lead to the largest enhancement in mechanical and rheological properties for various desired applications.

Bibliography

1. Chen, Q., Tudryn, G. J. & Colby, R. H. Ionomer dynamics and the sticky Rouse model. *J. Rheol.* **57**, 1441–1462 (2013).
2. Zhang, L., Brostowitz, N. R., Cavicchi, K. A. & Weiss, R. A. Perspective: Ionomer Research and Applications. *Macromol. React. Eng.* **8**, 81–99 (2014).
3. Massey, L. K. Chapter 17 - Ionomer. in *The Effects of UV Light and Weather on Plastics and Elastomers (Second Edition)* (ed. Massey, L. K.) 103–108 (William Andrew Publishing, 2007). doi:10.1016/B978-081551525-8.50021-X.
4. Cavicchi, K. A., Pantoja, M. & Cakmak, M. Shape memory ionomers. *J. Polym. Sci. Part B Polym. Phys.* **54**, 1389–1396 (2016).
5. Hasani-Sadrabadi, M. M. *et al.* Preparation and characterization of nanocomposite polyelectrolyte membranes based on Nafion® ionomer and nanocrystalline hydroxyapatite. *Polymer* **52**, 1286–1296 (2011).
6. Merlo, L., Ghielmi, A. & Arcella, V. FUEL CELLS – PROTON-EXCHANGE MEMBRANE FUEL CELLS | Membranes: Advanced Fluorinated. in *Encyclopedia of Electrochemical Power Sources* (ed. Garche, J.) 680–699 (Elsevier, 2009). doi:10.1016/B978-044452745-5.00930-8.
7. Otocka, E. P. & Kwei, T. K. Properties of Ethylene-Metal Acrylate Copolymers. 5 (1968).
8. Takahashi, T., Watanabe, J., Minagawa, K. & Koyama, K. Effect of ionic interaction on elongational viscosity of ethylene-based ionomer melts. *Polymer* **35**, 5722–5728 (1994).
9. Yan, F. Y., Gross, K. A., Simon, G. P. & Berndt, C. C. Mechanical and erosion properties of CaCO3-EMAA thermal sprayed coatings. *Polym. Eng. Sci.* **44**, 1448–1459 (2004).
10. Sakamoto, K., MacKnight, W. J. & Porter, R. S. Dynamic and steady-shear melt rheology of and ethylene-methacrylic acid copolymer and its salts. *J. Polym. Sci. Part -2 Polym. Phys.* **8**, 277–287 (1970).
11. Adi Eisenberg, Hird, B. & Moore, R. B. A new multiplet-cluster model for the morphology of random ionomers. *Macromolecules* **23**, 4098–4107 (1990).
12. MacKnight, W. J., McKenna, L. W., Read, B. E. & Stein, R. S. Properties of ethylene-methacrylic acid copolymers and their sodium salts. Infrared studies. *J. Phys. Chem.* **72**, 1122–1126 (1968).

13. Ward, T. C. & Tobolsky, A. V. Viscoelastic study of ionomers. *J. Appl. Polym. Sci.* **11**, 2403–2415 (1967).
14. Szajdzinska-Pietek, E., Wolszczak, M., Plonka, A. & Schlick, S. Fluorescence Studies of Self-Assembly in Aqueous Solutions of Poly(ethylene-co-methacrylic acid) Ionomers. *J. Am. Chem. Soc.* **120**, 4215–4221 (1998).
15. Grady, B. P., Goossens, J. G. P. & Wouters, M. E. L. Morphology of Zinc-Neutralized Maleated Ethylene−Propylene Copolymer Ionomers: Structure of Ionic Aggregates As Studied by X-ray Absorption Spectroscopy. *Macromolecules* **37**, 8585–8591 (2004).
16. Huang, H.-C. & Zacharia, N. S. Polyelectrolyte Multilayers and Complexes to Modify Secondary Interactions in Ethylene-co-methacrylic Acid Ionomers. *ACS Macro Lett.* **1**, 209–212 (2012).
17. Earnest, T. R. & Macknight, W. J. Effect of hydrogen bonding and ionic aggregation on the melt rheology of an ethylene–methacrylic acid copolymer and its sodium salt. *J. Polym. Sci. Polym. Phys. Ed.* **16**, 143–157 (1978).
18. Tierney, N. K. & Register, R. A. Ion Hopping in Ethylene−Methacrylic Acid Ionomer Melts As Probed by Rheometry and Cation Diffusion Measurements. *Macromolecules* **35**, 2358–2364 (2002).
19. Tachino, H. *et al.* Dynamic mechanical relaxations of ethylene ionomers. *Macromolecules* **26**, 752–757 (1993).
20. Lu, L. & Li, G. One-Way Multishape-Memory Effect and Tunable Two-Way Shape Memory Effect of Ionomer Poly(ethylene-co-methacrylic acid). *ACS Appl. Mater. Interfaces* **8**, 14812–14823 (2016).
21. Jr, S. J. K., Ward, T. C. & Oyetunji, Z. Self-Healing of Poly(Ethylene-co-Methacrylic Acid) Copolymers Following Projectile Puncture. *Mech. Adv. Mater. Struct.* **14**, 391–397 (2007).
22. Grady, B. P. Review and critical analysis of the morphology of random ionomers across many length scales. *Polym. Eng. Sci.* **48**, 1029–1051 (2008).
23. Farrell, K. V. Effects of Temperature on Aggregate Local Structure in a Zinc-Neutralized Carboxylate Ionomer. *Macromolecules* **33**, 7122–7126 (2000).
24. Nishioka, A., Takahashi, T., Masubuchi, Y., Takimoto, J. & Koyama, K. Melt rheology of ethylene ionomers blended with a small-molecule acid. *Polymer* **42**, 7907–7910 (2001).

25. Nishioka, A., Koda, T., Miyata, K., Murasawa, G. & Koyama, K. The Effects of Small Contents of Water on Melt Rheology for Ethylene-Methacrylic Zinc Ionomers. *Polym. J.* **40**, 350–353 (2008).
26. Tachino, H., Hara, H., Hirasawa, E., Kutsumizu, S. & Yano, S. Structure and properties of ethylene ionomers neutralized with binary metal cations. *Macromolecules* **27**, 372–378 (1994).
27. Xue, H., Bhowmik, P. & Schlick, S. Direct detection of ionic clustering in telechelic ionomers by DSC and ESR. *Macromolecules* **26**, 3340–3343 (1993).
28. Tierney, N. K. & Register, R. A. The Role of Excess Acid Groups in the Dynamics of Ethylene−Methacrylic Acid Ionomer Melts. *Macromolecules* **35**, 6284–6290 (2002).
29. Tomkovic, T. & Hatzikiriakos, S. G. Nonlinear rheology of poly(ethylene-co-methacrylic acid) ionomers. *J. Rheol.* **62**, 1319–1329 (2018).
30. Leibler, L., Rubinstein, M. & Colby, R. H. Dynamics of reversible networks. *Macromolecules* **24**, 4701–4707 (1991).
31. Mitsoulis, E. 50 Years of the K-BKZ Constitutive Relation for Polymers. *ISRN Polym. Sci.* **2013**, 1–22 (2013).
32. Kalista, S. J., Pflug, J. R. & Varley, R. J. Effect of ionic content on ballistic self-healing in EMAA copolymers and ionomers. *Polym. Chem.* **4**, 4910–4926 (2013).
33. Bhagabati, P. & Chaki, T. K. Compatibility study of chlorinated polyethylene/ethylene methacrylate copolymer blends using thermal, mechanical, and chemical analysis. *J. Appl. Polym. Sci.* **131**, (2014).
34. James, N. K., Ende, D. van den, Lafont, U., Zwaag, S. van der & Groen, W. A. Piezoelectric and mechanical properties of structured PZT–epoxy composites. *J. Mater. Res.* **28**, 635–641 (2013).
35. Kim, T.-H., Park, J. H., Lee, T.-W. & Park, O. O. Enhanced electroluminescence from a conjugated polymer/ionomer blend. *Polymer* **45**, 8567–8571 (2004).
36. Szabó, G., Kun, D., Renner, K. & Pukánszky, B. Structure, properties and interactions in ionomer/lignin blends. *Mater. Des.* **152**, 129–139 (2018).
37. Wu, W., Zhou, Y., Li, J. & Wan, C. Shape memory and self-healing behavior of styrene–butadiene–styrene/ethylene-methacrylic acid copolymer (SBS/EMAA) elastomers containing ionic interactions. *J. Appl. Polym. Sci.* **137**, 48666 (2020).

38. Zhou, N. C., Burghardt, W. R. & Winey, K. I. Blend Miscibility of Sulfonated Polystyrene Ionomers with Polystyrene: Effect of Counterion Valency and Neutralization Level. *Macromolecules* **40**, 6401–6405 (2007).
39. Natansohn, Almeria. & Eisenberg, Adi. Nuclear magnetic resonance studies of ionomers. 1. Interactions between poly(methyl methacrylate-co-4-vinylpyridine) and poly(styrene-co-styrenesulfonic acid) in dimethyl sulfoxide solution. *Macromolecules* **20**, 323–329 (1987).
40. Dow's PARALOID^{TM} impact modifiers enhance performance of Callaway golf balls. *Addit. Polym.* **2021**, 2–3 (2021).
41. Silva, P. A. P., Silva, A. B. da, Santos, J. P. F. & Oréfice, R. L. Self-healing polymer blend based on PETG and EMAA. *J. Appl. Polym. Sci.* **138**, 50148 (2021).
42. Datta, P., Guha, C. & Sarkhel, G. Effect of Na-ionomer on dynamic rheological, dynamic mechanical and creep properties of acrylonitrile styrene acrylate (ASA)/Na+1 poly (ethylene-co-methacrylic acid) ionomer blend. *Polym. Adv. Technol.* **25**, 1454–1463 (2014).
43. Balasubramanian, R., Park, S., Kim, S. S. & Lee, J. Studies on the thermal, mechanical, compatibility, and morphological properties of zinc-neutralized ethylene/methacrylic acid copolymer ionomer blend with m-aramid. *J. Thermoplast. Compos. Mater.* **33**, 1234–1247 (2020).
44. Miwa, Y., Koike, M., Kohbara, Y. & Kutsumizu, S. Effects of fatty acids having different alkyl tail lengths on rigidness of the shell region surrounding an ionic core and mechanical properties of poly(ethylene-co-methacrylic acid) ionomer/fatty acid blends. *Polymer* **197**, 122495 (2020).
45. Vanhoorne, P. & Register, R. A. Low-Shear Melt Rheology of Partially-Neutralized Ethylene−Methacrylic Acid Ionomers. *Macromolecules* **29**, 598–604 (1996).
46. Grady, B. P. Effect of Coneutralization on Internal Aggregrate Structure in Ethylene-Based Ionomers. *Macromolecules* **32**, 2983–2988 (1999).
47. Nishio, M., Nishioka, A., Taniguchi, T. & Koyama, K. Rheological properties of ethylene ionomer neutralized with binary metal cation. *Polymer* **46**, 261–266 (2005).
48. Loo, Y.-L., Wakabayashi, K., Huang, Y. E., Register, R. A. & Hsiao, B. S. Thin crystal melting produces the low-temperature endotherm in ethylene/methacrylic acid ionomers. *Polymer* **46**, 5118–5124 (2005).

49. Harlin, A. & Ferenets, M. 13 - Introduction to conductive materials. in *Intelligent Textiles and Clothing* (ed. Mattila, H. R.) 217–238 (Woodhead Publishing, 2006). doi:10.1533/9781845691622.3.217.
50. Trigg, E. B. & Winey, K. I. Nanoscale layers in polymers to promote ion transport. *Mol. Syst. Des. Eng.* **4**, 252–262 (2019).
51. Reynolds, P. J. A Surlyn® Ionomer as a Self-Healing and Self-Sensing Composite. (University of Birmingham, 2011).
52. Reflux | Laboratory techniques. https://biocyclopedia.com/index/chem_lab_methods/reflux.php.
53. Höhne, G. W. H., Hemminger, W. F. & Flammersheim, H.-J. Introduction. in *Differential Scanning Calorimetry* (eds. Höhne, G. W. H., Hemminger, W. F. & Flammersheim, H.-J.) 1–7 (Springer, 2003). doi:10.1007/978-3-662-06710-9_1.
54. Molnar, A. & Adi Eisenberg. Miscibility of polyamide-6 with lithium or sodium sulfonated polystyrene ionomers. *Macromolecules* **25**, 5774–5782 (1992).
55. Kutsumizu, S. *et al.* Investigation of Microphase Separation and Thermal Properties of Noncrystalline Ethylene Ionomers. 2. IR, DSC, and Dielectric Characterization. *Macromolecules* **33**, 9044–9053 (2000).
56. Smith, B. C. *Fundamentals of Fourier transform infrared spectroscopy*. (CRC Press, 1996).
57. Aho, J., Boetker, J. P., Baldursdottir, S. & Rantanen, J. Rheology as a tool for evaluation of melt processability of innovative dosage forms. *Int. J. Pharm.* **494**, 623–642 (2015).
58. Snijkers, F. & Vlassopoulos, D. Cone-partitioned-plate geometry for the ARES rheometer with temperature control. *J. Rheol.* **55**, 1167–1186 (2011).
59. Chapter 4 - Normal Stresses. in *Rheology Series* (eds. Barnes, H. A., Hutton, J. F. & Walters, K.) vol. 3 55–73 (Elsevier, 1989).
60. Tomkovic, T., Mitsoulis, E. & Hatzikiriakos, S. G. Contraction flow of ionomers. *J. Non-Newton. Fluid Mech.* **262**, 131–141 (2018).
61. Tomkovic, T., Mitsoulis, E. & Hatzikiriakos, S. G. Contraction flow of ionomers and their corresponding copolymers: Ionic and hydrogen bonding effects. *Phys. Fluids* **31**, 033102 (2019).
62. Zuliki, M., Zhang, S. (张世岭), Tomkovic, T. & Hatzikiriakos, S. G. Capillary flow of sodium and zinc ionomers. *Phys. Fluids* **32**, 023106 (2020).

63. Zuliki, M., Zhang, S., Nyamajaro, K., Tomkovic, T. & Hatzikiriakos, S. G. Rheology of sodium and zinc ionomers: Effects of neutralization and valency. *Phys. Fluids* **32**, 023104 (2020).
64. Huang, C., Wang, C., Chen, Q., Colby, R. H. & Weiss, R. A. Reversible Gelation Model Predictions of the Linear Viscoelasticity of Oligomeric Sulfonated Polystyrene Ionomer Blends. *Macromolecules* **49**, 3936–3947 (2016).
65. Kazatchkov, I. B. Influence of molecular structure on rheological and processing behaviour of molten polymers. (The University of British Columbia (Canada), 1999).
66. Rolón-Garrido, V. H. & Wagner, M. H. The damping function in rheology. *Rheol. Acta* **48**, 245–284 (2009).
67. *Tensile testing*. (ASM International, 2004).
68. Huang, H.-C. & Zacharia, N. S. Polyelectrolyte Multilayers and Complexes to Modify Secondary Interactions in Ethylene-co-methacrylic Acid Ionomers. *ACS Macro Lett.* **1**, 209–212 (2012).
69. Xue, H., Bhowmik, P. & Schlick, S. Direct detection of ionic clustering in telechelic ionomers by DSC and ESR. *Macromolecules* **26**, 3340–3343 (1993).
70. Pregi, E., Kun, D., Wacha, A. & Pukánszky, B. The role of ionic clusters in the determination of the properties of partially neutralized ethylene-acrylic acid ionomers. *Eur. Polym. J.* **142**, 110110 (2021).
71. Lee, J. A., Kontopoulou, M. & Parent, J. S. Rheology and Physical Properties of Polyethylene/Polyethylene-Ionomer Blends and their Clay Nanocomposites. *Macromol. Rapid Commun.* **28**, 210–214 (2007).
72. Miwa, Y., Kohbara, Y., Furukawa, H. & Kutsumizu, S. The effects of local glass transition temperatures of ionic core–shell structures on the tensile behavior of sodium-neutralized poly(ethylene-co-methacrylic acid) ionomer/lauric acid blends. *Polymer* **148**, 303–309 (2018).

Appendix

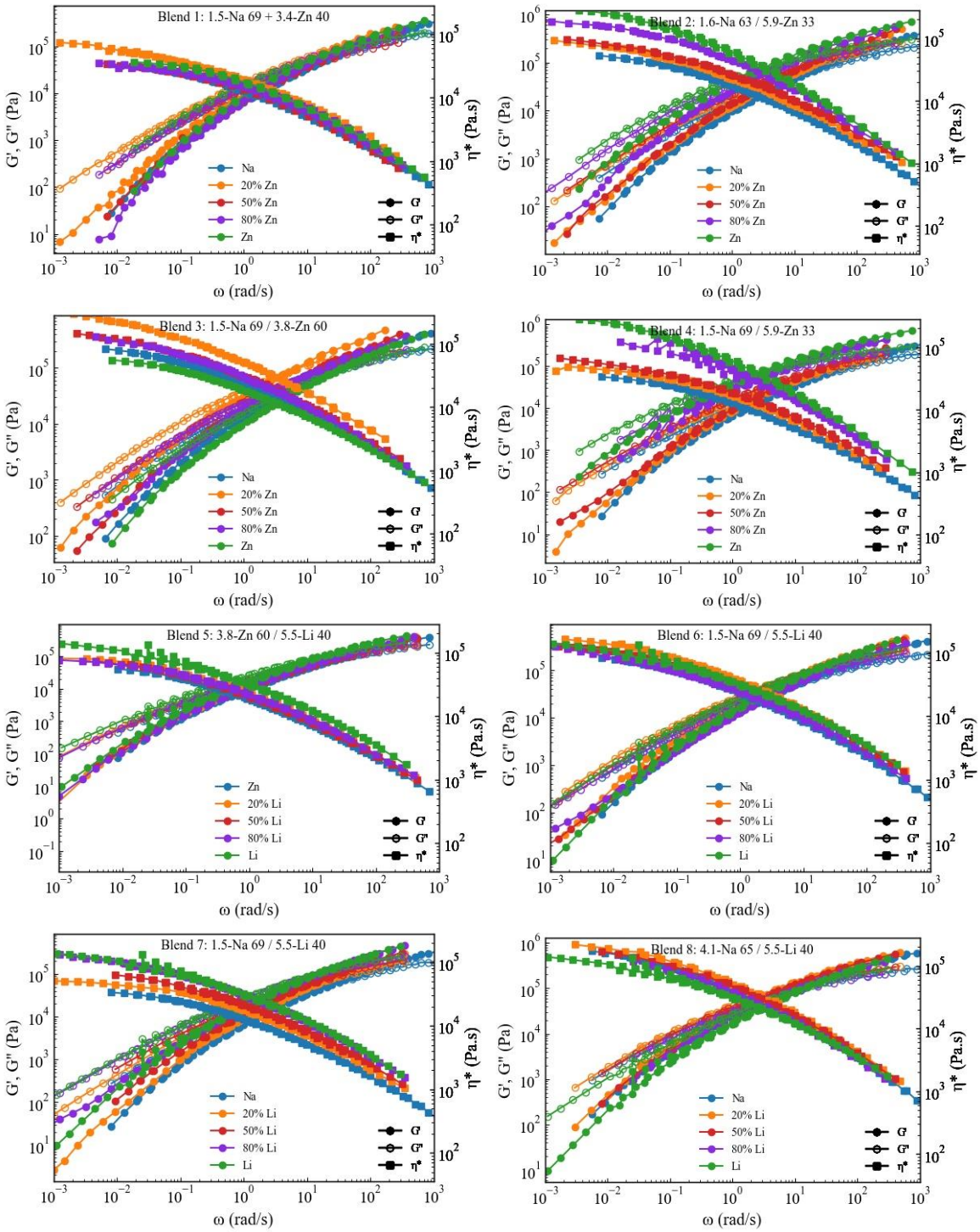

Figure A 1. Frequency sweep curves for all blends at 140ºC, 5% strain using cone-and-plate geometry. Filled circles represent storage modulus, open circles represent loss modulus, squares represent complex viscosity.

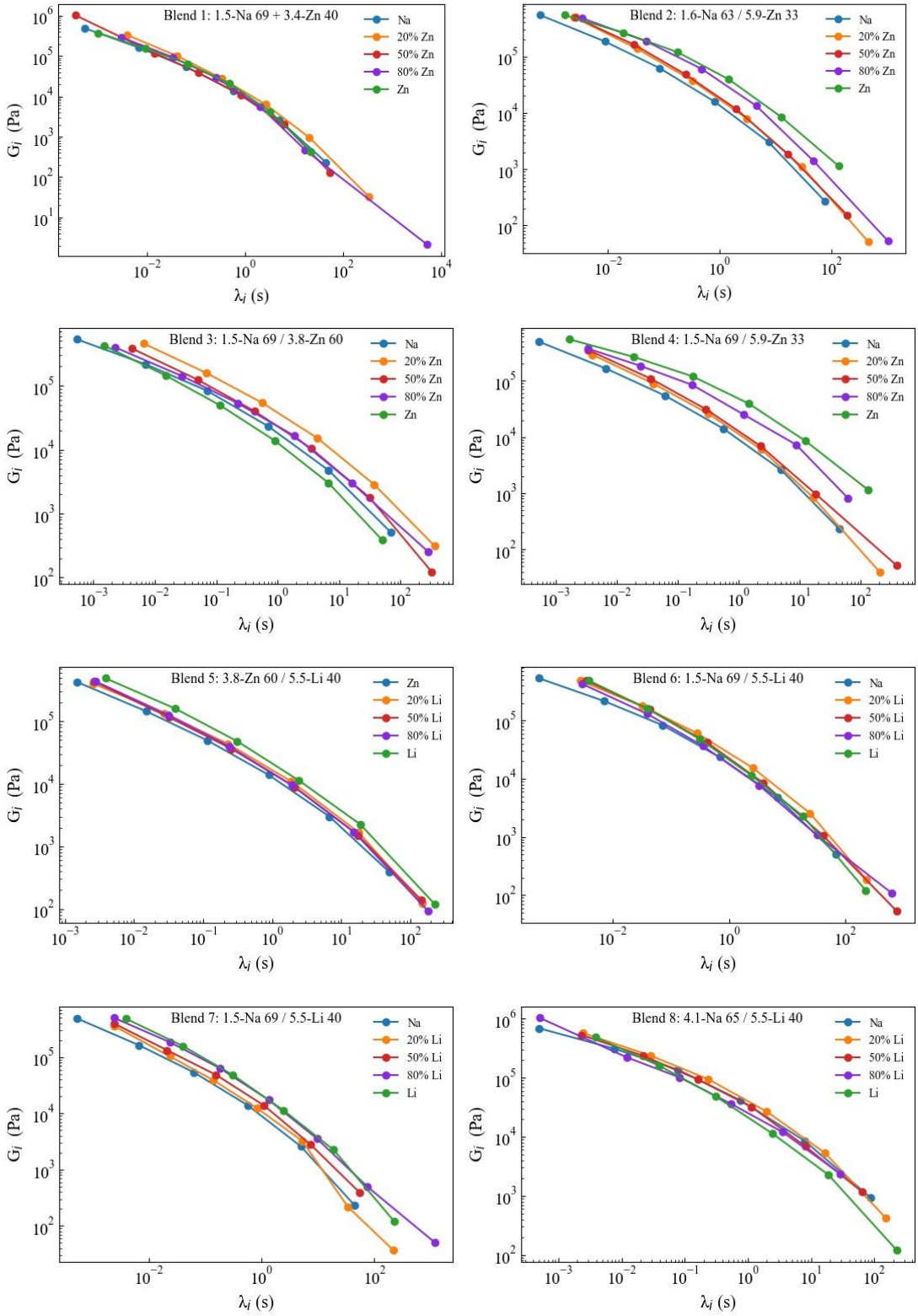

Figure A 2. Maxwell relaxation spectrum obtained through Maxwell fitting of the frequency sweep mastercurve at 120ºC, 140ºC, 160ºC, and 180ºC. Six relaxation modes accurately fit experimental results.

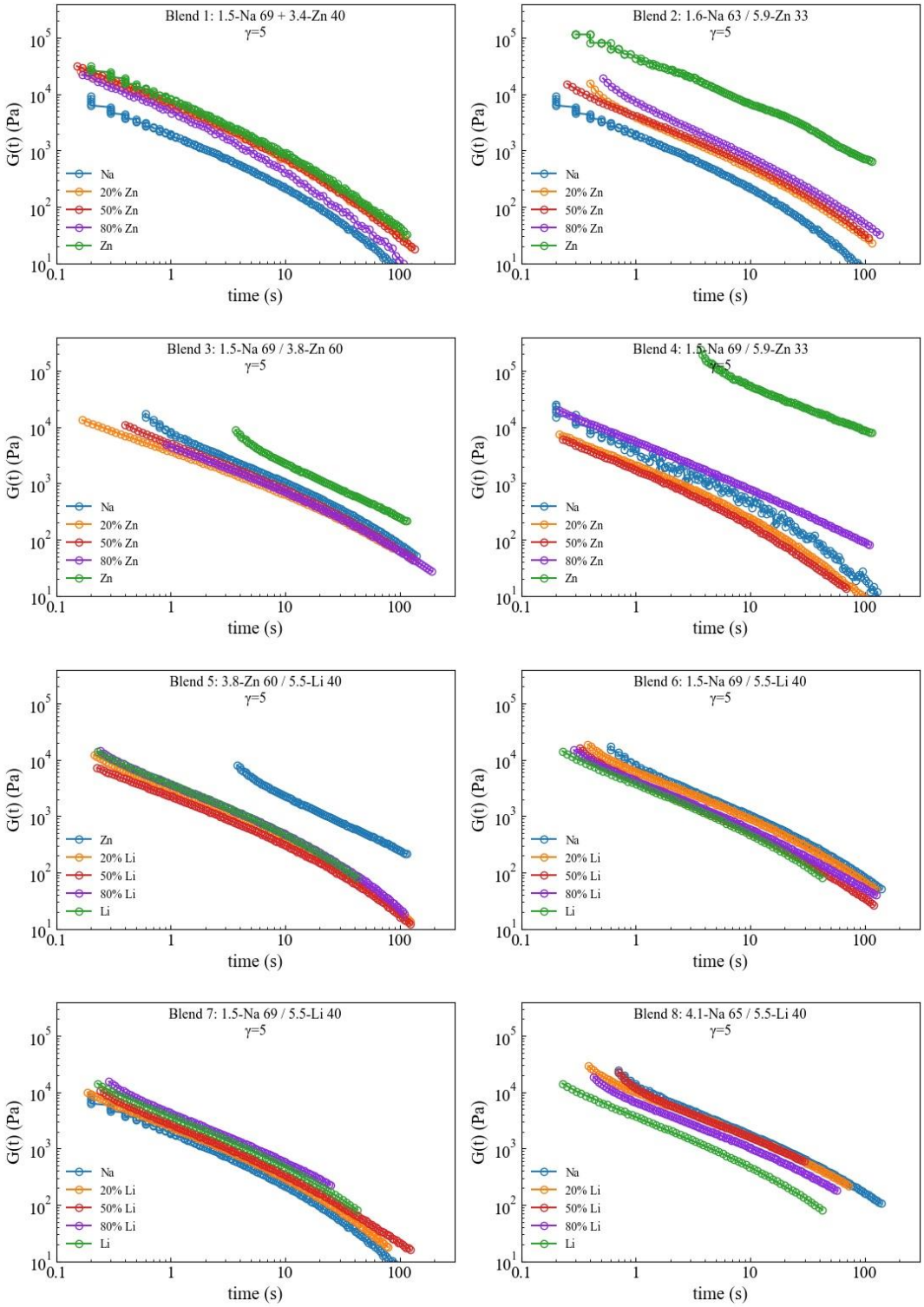

Figure A 3. Relaxation modulus for all blends measured using cone-and-plate geometry at 140oC and strain amplitude of 5 (500%)

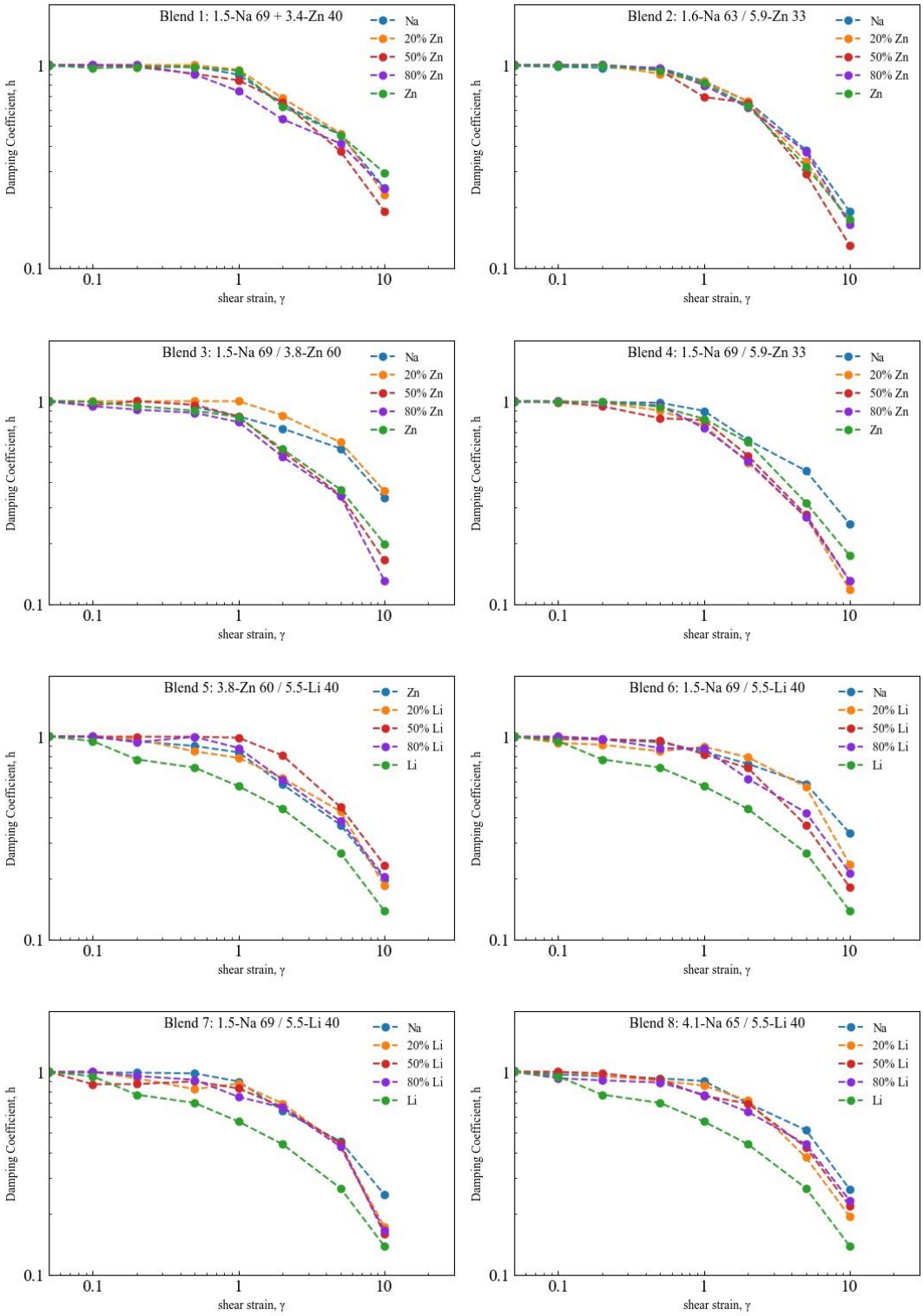

Figure A 4. Damping coefficient vs strain calculated as the ratio between the relaxation modulus at each strain and the relaxation modulus at a strain of 0.05 (5%) which lies in the linear viscoelastic region.

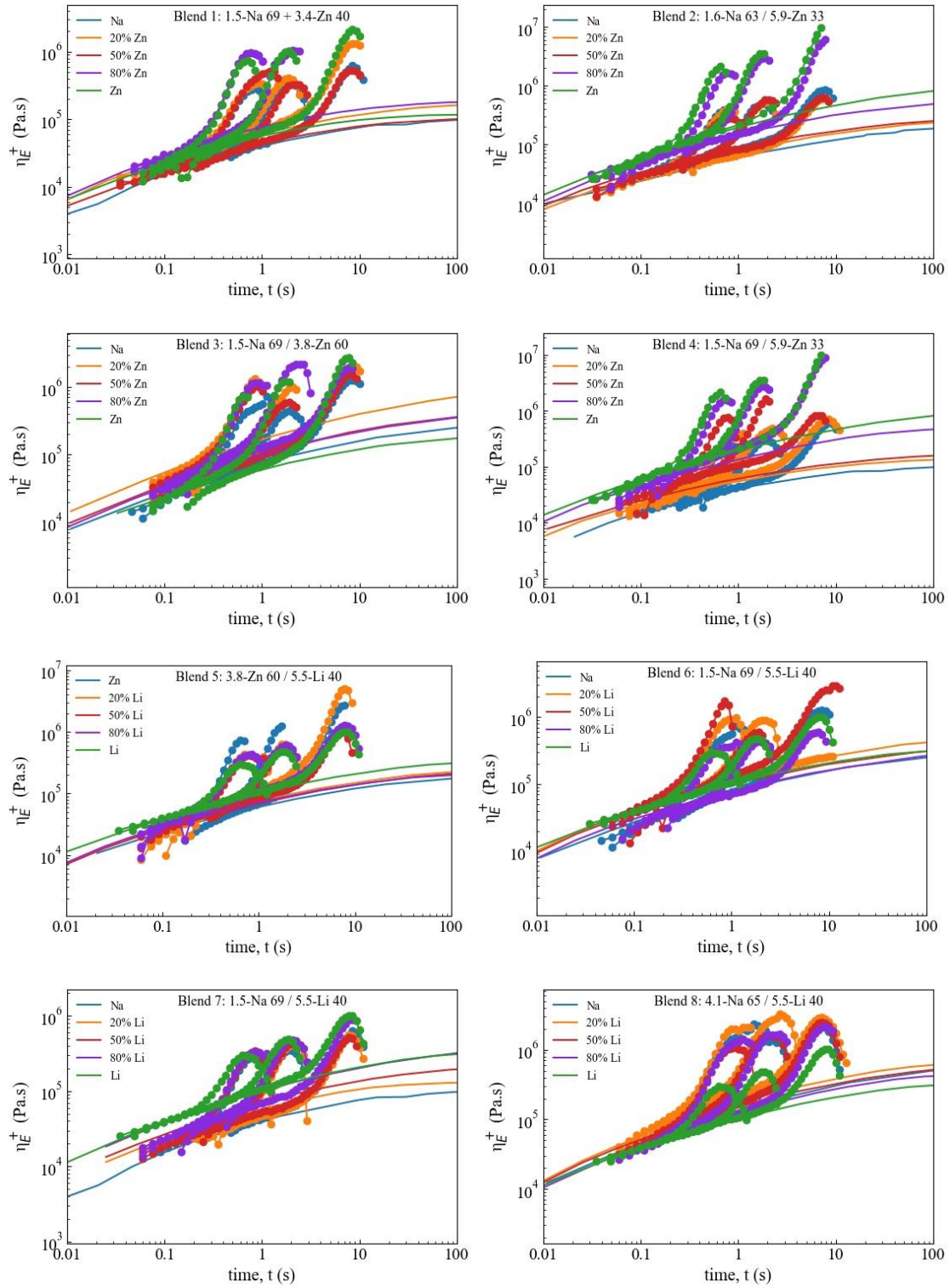

Figure A 5. Extensional viscosity vs time for all blends measured using the Sentmanat Extensional Rheology (SER) fixture at Hencky strain rates of 0.5, 2, and 5 1/s at 140ºC.

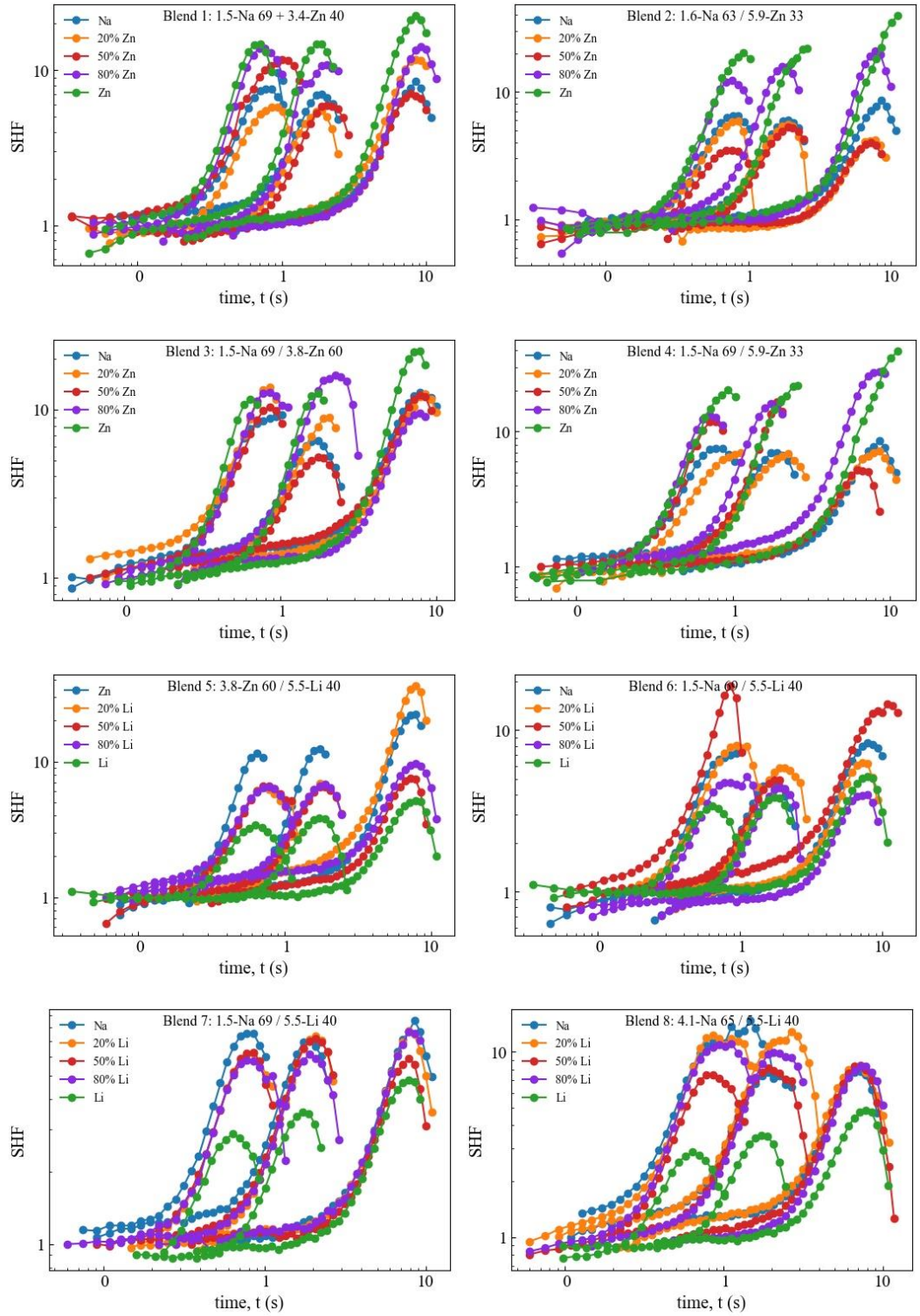

Figure A 6. Strain Hardening Factor (SHF) vs time for all blends calculated by dividing the extensional viscosity by the linear viscoelastic envelope (3η+).

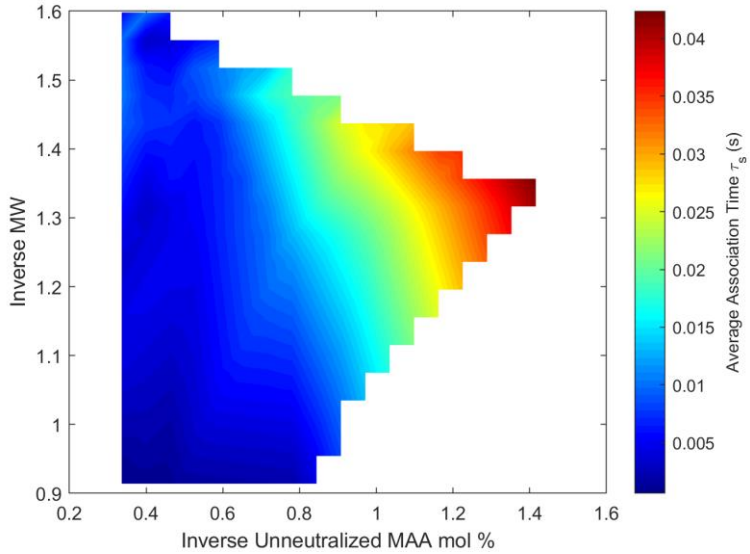

Figure A 7. 3D Colormap of the components of MW-normalized neutralization (NMW), inverse MW and unneutralized MAA mol % showing a correlation between high average association time, moderate inverse MW, and high levels of neutralization.

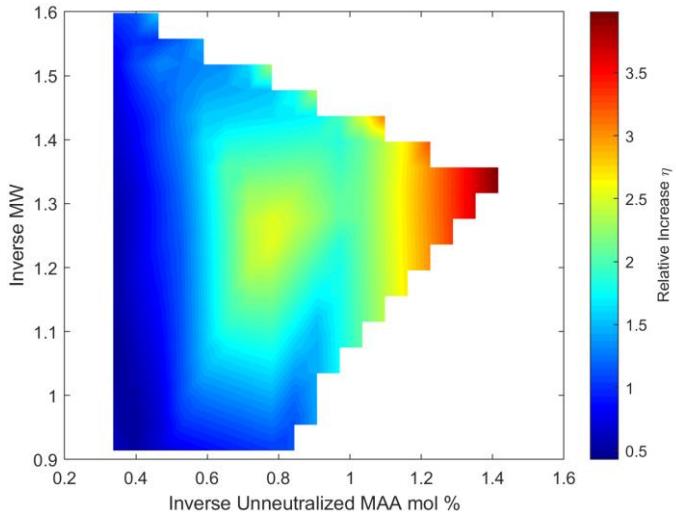

Figure A 8. 3D colormap of the components of NMW showing a higher relative increase in zero-shear viscosity at moderate values of inverse MW and high levels of neutralization

Table A 1. Summary of blend properties including analysis of molecular-weight normalized neutralization values

	mol% MAA	Neutralization %	Mw (g/mol)	Neutralized MAA mol %	Zs	τ rep (s)	τ_s association time (s)	1/ $MW_{combined}$	η_o (kPa.s)	N_{MW}	Rel. Inc. η_o	E (MPa)	Rel. Inc. E
B1 Na 1802	7.2	65	65200	4.68	35	44.60	6.5 x 10^-4	1.53	35.87			0.78	
B1 20%	6.44	60	64640	4.02	29	338.20	7.4 x 10^-3	1.55	61.93	0.64	1.69	1.30	1.57
B1 50%	5.3	52.5	63800	3.02	21	53.00	2.3 x 10^-3	1.57	34.67	0.69	0.92	1.93	2.13
B1 80%	4.16	45	62960	2.02	14	16.00	1.6 x 10^-3	1.59	41.73	0.74	1.08	1.38	1.41
B1 Zn 9650	3.4	40	62400	1.36	10	22.10	4.3 x 10^-3	1.60	39.26			1.03	
B2 Na 1605	1.6	63	114500	1.01	13	75.00	4.3 x 10^-3	0.87	55.40			13.78	
B2 20%	2.46	57	114440	1.20	19	29.80	8.9 x 10^-4	0.87	92.18	0.69	0.85	12.68	0.89
B2 50%	3.75	48	114350	1.48	24	16.00	2.9 x 10^-4	0.87	96.87	0.38	0.51	8.68	0.58
B2 80%	5.04	39	114260	1.76	26	47.00	7.2 x 10^-4	0.88	203.78	0.27	0.76	10.88	0.69
B2 Zn 9120	5.9	33	114200	1.95	26	133.00	2.0 x 10^-3	0.88	322.00			16.35	
B3 Na 1601	1.5	69	72500	1.04	9	69.20	1.5 x 10^-2	1.38	86.40			8.28	
B3 20%	1.96	67.2	74380	1.28	11	359.09	4.4 x 10^-2	1.34	343.72	1.99	4.26	24.00	2.93
B3 50%	2.65	64.5	77200	1.66	15	323.75	2.1 x 10^-2	1.30	144.41	1.31	2.00	21.45	2.65
B3 80%	3.34	61.8	80020	2.03	19	277.90	1.1 x 10^-2	1.25	169.55	0.95	2.66	18.27	2.30
B3 Zn 1650	3.8	60	81900	2.28	22	50.10	1.5 x 10^-3	1.22	58.00			7.88	

	mol% MAA	Neutralization %	Mw (g/mol)	Neutralized MAA mol %	Zs	τ rep (s)	τ_s association time (s)	$1/MW_{combined}$	η_o (kPa.s)	N_{MW}	Rel. Inc. η_o	E (MPa)	Rel. Inc. E
B4 Na 1802	7.2	65	65200	4.68	35	44.60	6.5 x 10^-4	1.53	33.90			19.35	
B4 20%	6.94	58.6	75000	4.13	35	207.15	2.6 x 10^-3	1.33	48.84	0.48	0.53	6.64	0.38
B4 50%	6.55	49	89700	3.31	33	391.33	4.6 x 10^-3	1.11	69.94	0.34	0.39	4.56	0.30
B4 80%	6.16	39.4	104400	2.49	29	62.50	8.2 x 10^-4	0.96	165.00	0.26	0.62	5.40	0.43
B4 Zn 9120	5.9	33	114200	1.95	26	133.80	2.1 x 10^-3	0.88	322.00			10.73	
B5 Zn 1650	3.8	60	81900	2.28	22	50.10	1.5 x 10^-3	1.22	58.00			7.93	
B5 20%	4.13	56	77520	2.26	21	147.91	5.2 x 10^-3	1.29	85.34	0.69	1.22	5.39	0.67
B5 50%	4.625	50	70950	2.23	19	144.65	6.7 x 10^-3	1.41	81.31	0.59	0.92	8.03	0.99
B5 80%	5.12	44	64380	2.20	17	180.61	1.1 x 10^-2	1.55	78.05	0.53	0.73	7.31	0.88
B5 Li 7940	5.45	40	60000	2.18	15	225.38	1.9 x 10^-2	1.67	119.00			8.35	
B6 Na 1601	1.5	69	72500	1.04	9	69.20	1.5 x 10^-2	1.38	86.40			8.28	
B6 20%	2.29	63.2	70000	1.26	12	228.00	2.8 x 10^-2	1.43	165.00	1.39	1.78	17.94	2.42
B6 50%	3.475	54.5	66250	1.61	15	115.00	9.7 x 10^-3	1.51	132.89	0.81	1.29	16.53	2.71
B6 80%	4.66	45.8	62500	1.95	16	191.00	1.5 x 10^-2	1.60	128.00	0.59	1.14	8.89	1.86
B6 Li 7940	5.45	40	60000	2.18	15	225.00	1.9 x 10^-2	1.67	119.00			3.90	

	mol% MAA	Neutralization %	Mw (g/mol)	Neutralized MAA mol %	Zs	τ rep (s)	τ_s association time (s)	$1/MW_{combined}$	η_o (kPa.s)	N_{MW}	Rel. Inc. η_o	E (MPa)	Rel. Inc. E
B7 Na 1802	7.2	65	65200	4.68	35	44.60	6.5 x 10^-4	1.53	33.90			15.78	
B7 20%	6.85	60	64160	4.18	31	175.00	3.4 x 10^-3	1.56	51.24	0.58	1.01	16.83	1.26
B7 50%	6.325	52.5	62600	3.43	24	54.00	1.7 x 10^-3	1.60	71.40	0.55	0.93	15.11	1.54
B7 80%	5.8	45	61040	2.68	19	75.00	4.3 x 10^-3	1.64	147.30	0.53	1.44	11.40	1.82
B7 Li 7940	5.45	40	60000	2.18	15	225.38	1.9 x 10^-2	1.67	119.00			3.90	
B8 Na 1707	4.1	65	71000	2.67	22	86.90	3.0 x 10^-3	1.41	176.00			2.37	
B8 20%	4.37	60	68800	2.57	21	151.36	6.0 x 10^-3	1.45	238.57	0.81	1.45	4.02	1.50
B8 50%	4.775	52.5	65500	2.42	19	64.21	3.2 x 10^-3	1.53	196.76	0.65	1.33	5.58	1.78
B8 80%	5.18	45	62200	2.28	17	28.96	1.9 x 10^-3	1.61	146.48	0.55	1.12	6.64	1.85
B8 Li 7940	5.45	40	60000	2.18	15	225.38	1.9 x 10^-2	1.67	119.00			3.90	